Fractures of the Eumeralla Formation, Otway Ranges, Australia: Timing and Generation of Fluid Flow

Thesis submitted in accordance with the requirements of the University of Adelaide for an Honours Degree in Geology

Lachlan Furness

November 2016

THE UNIVERSITY of ADELAIDE

FRACTURES OF THE EUMERALLA FORMATION, OTWAY RANGES, AUSTRALIA: TIMING AND GENERATION OF FLUID FLOW

ABSTRACT

Over 261 naturally occurring fractures were recorded from 10 field locations in the Otway Ranges, Victoria, Australia. Fractures were sampled from the upper Jurassic – lower Cretaceous Eumeralla Formation, a volcanogenic sandstone. Eight Fracture Sets were recorded with defined orientations. Twenty-seven fracture samples from across the Otway Ranges were thin sectioned and analysed using an optical microscope and Scanning Electron Microscope (SEM). Host rock and fracture petrography were determined, including identification of host rock and fracture cement mineral compositions, along with fracture specific textures, such as calcite twinning, crack-seal textures, cataclastic deformation and cross-cutting cements.

Siderite cements are observed to be present in all fracture sets and imply the presence of fluid flow during all periods of deformation, from lower Cretaceous extension to NW – SE Miocene compression. The addition of calcite cements in Fracture Sets One, Fracture Set Two, Fracture Set Four, Fracture Set Five and Fracture Set Seven indicate two periods of enhanced calcite and siderite fluid flow predominantly during times of NW - SE compression in the mid-Cretaceous and Miocene.

KEYWORDS

Otway Basin, Fracture Cements, Eumeralla Formation, Structural Permeability, Fluid Flow, Fracture Mechanics

TABLE OF CONTENTS

.

LIST OF FIGURES AND TABLES

1.0 INTRODUCTION

The geochemical signature and textures of cemented fractures in sedimentary basins can express phases of fluid flow, permeability, thermal history, stress field changes, and tectonic evolution of a basin through time (Laubach et al., 2004a; Bons et al., 2012). Fluctuating stress states that occur throughout the history of a basin may result in fluid migration, seismic valving and pumping through fault and fracture meshes (Sibson, 2000; Krassay et al., 2004; Sibson, 2004). Fluid flow within sedimentary basins take place when the lithosphere experiences stress from extensional and compressional forces through loading of sediments, mantle driven mechanics, and compressional forces resulting in inversion of buried rocks (Krassay et al., 2004; Osborne and Swarbrick, June 1997). The accompanying fluid cementation of fractures identified in the Otway Basin have textures that display crack seal events that involve cement fill with each increment of fracture opening, mineral bridges and cross-cutting fracture cements (Laubach, 2003; Laubach et al., 2004a; Laubach et al., 2004b; Laubach et al., 2010). Further study is required as prediction and understanding of fracture networks and fracture characteristics like fracture cements is vital for unconventional hydrocarbon systems, geothermal energy, mineral and hydro industries which rely on the secondary permeability of low porosity systems (English, 2012). The Otway Basin is interpreted to have experienced multiple stress field changes from extensional rifting in the lower Cretaceous to compression, exhumation and uplift in the Miocene (Hill et al., 1995; Krassay et al., 2004). Fracture fills in the Otway Basin have been observed to consists of siderite, quartz and calcite and initial studies at limited locations demonstrate a complex fracture growth and fluid flow history in the Otway Basin (Sage, 2013). In this paper, I describe the structural measurements of fracture cements recorded during

field work. The petrological mineral composition and textures of fracture cements collected in the Otway Ranges. This is accomplished directly from the use of the optical microscope and Scanning Electron Microscope (SEM). I then discuss the relative timing of fracture sets interpreted, episodes of fluid flow in these fracture sets, timing of calcite and siderite cements and the implications fracture cements have on permeability in the Otway Ranges.

2.0 BACKGROUND

THE OTWAY BASIN

The Otway Basin is a continuous NW – SE trending rift basin that includes onshore and offshore parts of South Australia, Victoria and northern Tasmanian waters (Figure 1) (Krassay et al., 2004). The Otway Basin is a rift system along Australia's Southern Margin and is part of a group of basin's related to the upper Jurassic to lower Cretaceous continental separation of Australia and Antarctica (Figure 1). The evolution of the now passive margin Otway Basin spans 150 million years, and encompasses multiple phases of tectonic rifting, sagging, uplift and inversion from the Upper Jurassic to Miocene (Willcox and Stagg, 1990; Williamson et al., 1990; Hill et al., 1994; Hill et al., 1995). The Otway Basin has been extensively researched and been intensively explored for hydrocarbon reserves. Approximately 200 wells have been drilled with over 35,000km of 2D seismic lines offshore and onshore (Geoscience Australia). Five onshore production wells are currently in operation in Victoria (Tassone, 2014).

2.1 Geological Setting of the Otway Ranges

The Otway Ranges are situated in the eastern part of the Otway Basin, 162km south-west of Melbourne (Figure 1). The Otway Ranges experienced extensively more up-lift than western sectors of the basin (Hill et al., 1994). The main rocks that outcrop in the Otway Ranges are the lower Cretaceous, Eumeralla Formation which is part of the Otway Group, and the Eocene- Oligocene Nirranda Group sediments (Krassay et al., 2004) (Figure 2 an Figure 4).

2.2 Basin Evolution and Tectonic Setting of the Otway Ranges

Five tectonic phases characterise the history of the Otway Ranges (Figure 3). The first involving the initial rifting in the Otway Ranges commenced in the upper – Jurassic to lower - Cretaceous with debated extensional directions bearing NE-SW, NW-SE and N-S (Willcox and Stagg, 1990; Williamson et al., 1990; Hill et al., 1994; Hill et al., 1995; Perincek.D and C.D, 1995; Miller et al., 2002; Holford et al., 2014). It was during the lower-Cretaceous when the Eumeralla Formation was deposited, with large amounts of volcanoclastic sediments from subduction of the Pacific plate in the east accumulating within the formation (Willcox and Stagg, 1990; Krassay et al., 2004). During the mid-Cretaceous the eastern regions of the Otway Basin experienced NW –SE compression. At this time the Otway Ranges uplifted from thermal uplift linked to the break-up of the two continents (Hill et al., 1994). At the cessation of rapid uplift of the Otway Ranges, there was renewed N-S to oblique upper-Cretaceous rifting. This rifting stopped short of Tasmania and passed SW of Tasmania, effectively making the Bass Straight and the Torquay sub-basin failed rifts (Hill et al., 1995; Briguglio et al., 2015). Oceanic crust was first to form in the Great Australian Bight and propagated SE into the Otway Basin. Oceanic crust did not form in the Otway Basin region until the middle Eocene,

reinforcing the hypothesis of proposed slow sea-floor spreading during this period. Beginning in the middle Eocene fast sea-floor spreading commenced which resulted in rapid subsidence and subsequent marine transgression of the Otway Basin including the Otway Ranges. The marine transgression continued until the beginning of the Miocene to present-day where renewed NW – SE compression is observed (Krassay et al., 2004). This compression is argued to have reactivated normal faults created during the tectonic extension phases of the Otway Ranges and promoted folding, uplift and inversion of the Otway Ranges (Lyon et al., 2007; Holford et al., 2011a). The compressional regime is a result of arc collision of Australia and SE Asia in the north, ridge push from the mid-ocean ridge in the south and relative tectonic plate movement along the New Zealand tectonic plate boundary (Lyon et al., 2007).

2.3 Eumeralla Formation (Otway Group)

The Eumeralla Formation was deposited during the lower Cretaceous encompassing the initial rifting of Antarctica and Australia. The formation experiences all tectonic episodes of the Otway Basin and crops out extensively in the Otway Ranges (Duddy, 2003; Krassay et al., 2004). For this reason, it is an exceptional natural laboratory to study the fluid flow history of the Otway Basin. The Eumeralla Formation is the most homogenous and thickest rock unit in the Otway Basin with a thickness of approximately 3km (Duddy, 2003). All lithological members are composed of sand and large concentrations of volcanogenic detritus from rift related volcanism which is characteristic of the Eumeralla Formation (Duddy, 2003). Due to this, the Eumeralla Formation has large quantities of plagioclase and other altered volcanic rock fragments such as siderite and albite (Duddy, 2003). The depositional environment of the Eumeralla Formation is debated; it is often regarded as having been deposited in a low

energy river system. Whereas others have suggested that the Eumeralla Formation was deposited in a high energy non-marine fluvial system (Duddy, 2002; Krassay et al., 2004; Briguglio et al., 2015).

2.4 Diagenesis of Eumeralla Formation Otway Ranges

The Eumeralla Formation underwent rapid burial with parts of the Otway Ranges reaching depths of almost five kilometres in roughly twenty million years during the lower-Cretaceous (Tassone, 2014). Diagenesis began immediately after burial resulting in sandstones within the formation receiving large-scale destruction of permeability and porosity at only 1.5km depth, resulting in drastically reduced hydrocarbon reservoir quality (Duddy, 1997). After burial, extensive diagenesis occurred through dissolution of volatile volcanogenic sediments, such as olivine and orthopyroxene, by existing fresh pore water (Duddy, 2003). At 10m burial depth grains were coated in chlorite and smectite drastically reducing pore space. At a few 100's m depth before significant compaction began, precipitation of pore filling calcite and siderite from volcanogenic sediments occurred baring manganese (Duddy, 2002). At 1.5km's depth and at temperatures of 70°C calcic plagioclase and k – rich feldspar is albitised in reaction with marine sodic fluids (Duddy, 2002).

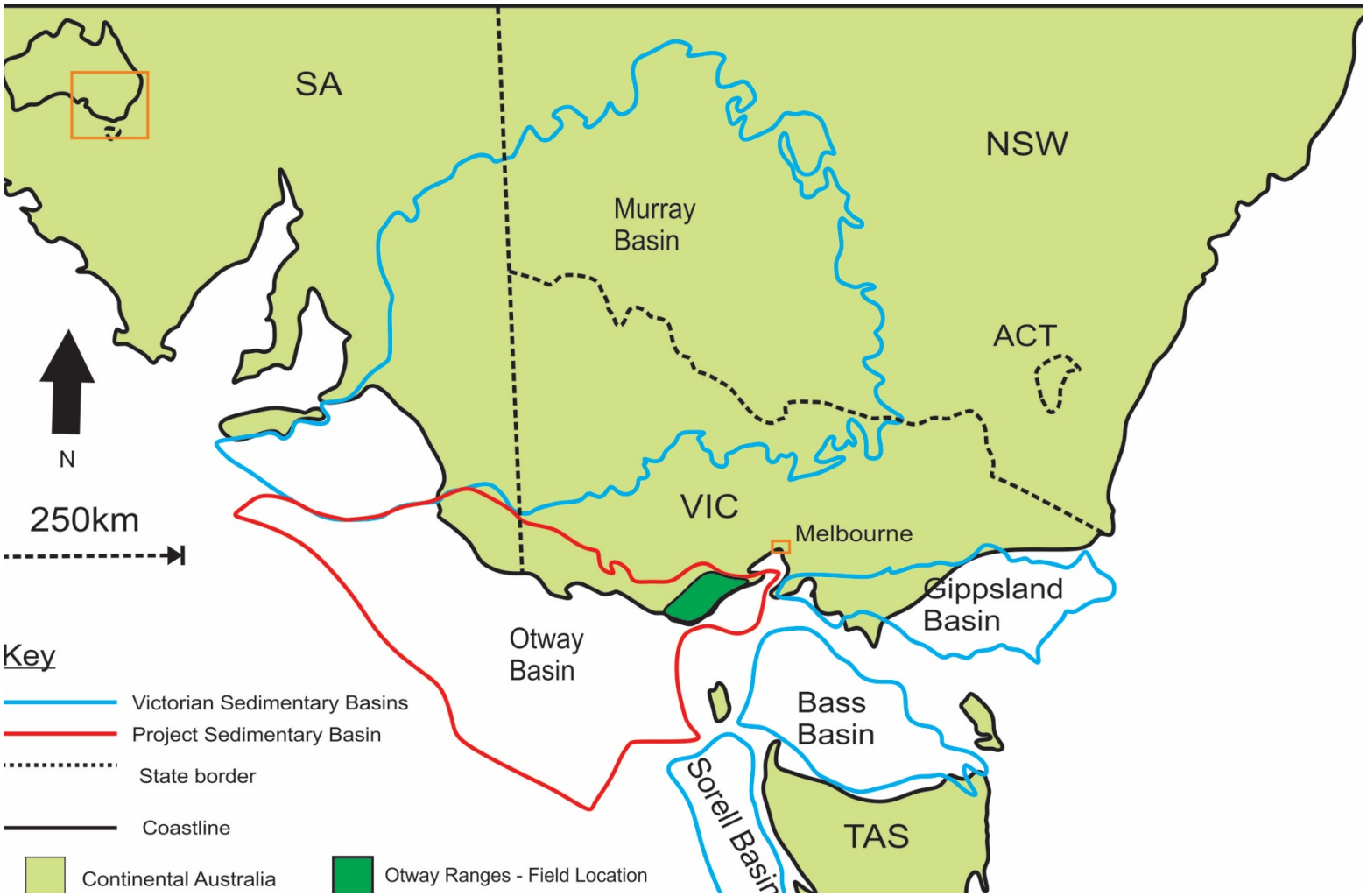

Figure 1. Geological setting of the Otway Basin. Displaying associated locations of all south eastern Australian sedimentary basins related to the rifting of Australia and Antarctica (Adapted from Geoscience Australia, 2016)

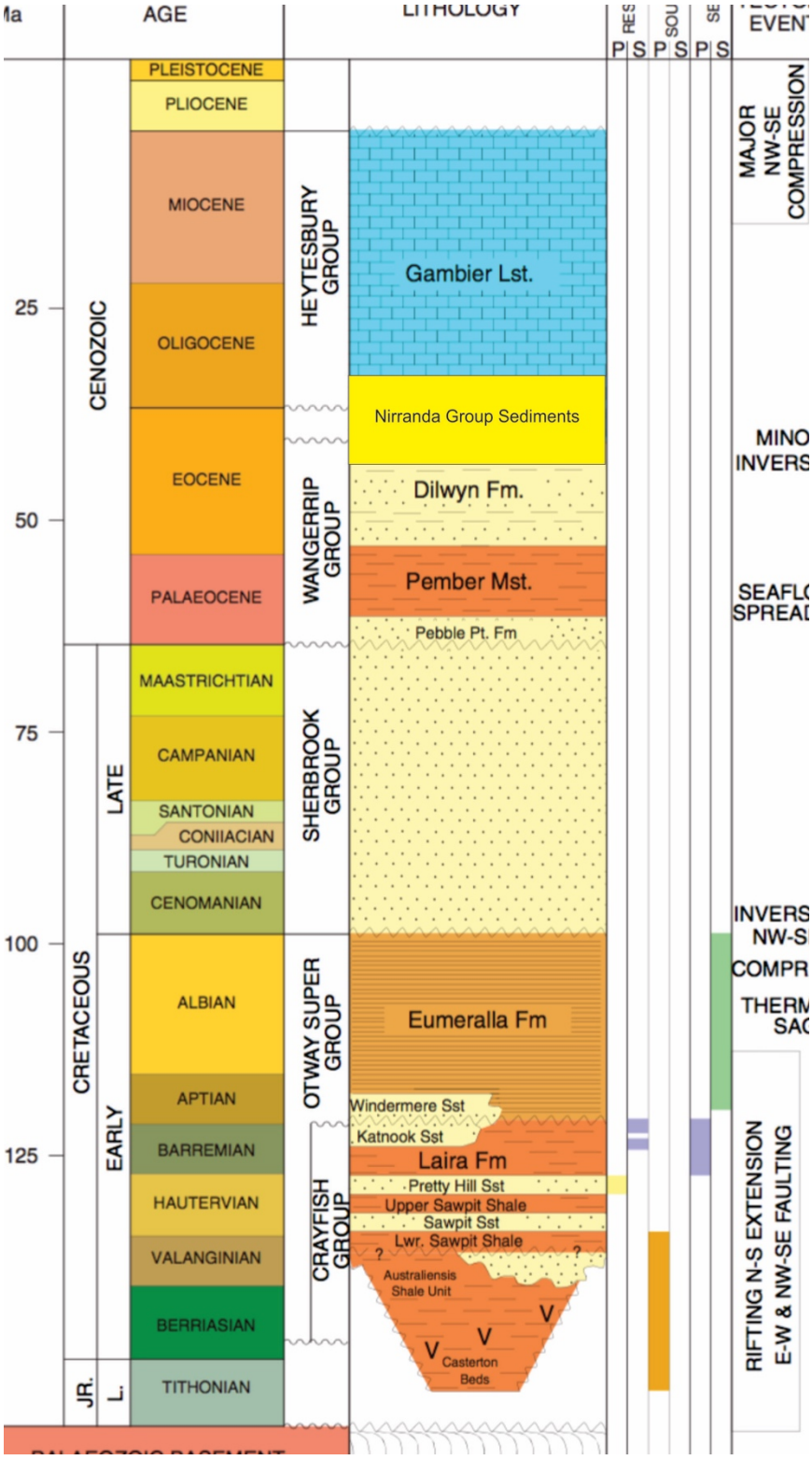

Figure 2. Chronostratigraphy column of Otway Basin including major tectonic events (Bailey et al., 2014), modified from (Lyon et al., 2007).

2.5 Fault Types Observed in the Otway Ranges

A normal fault involves the hanging wall sliding downwards relative to the footwall along the orientation of the fault plane. The orientation of the three principal stresses consists of maximum principal stress σ_1 being vertical, minimum principal stress σ_3 ninety degrees from strike of fault and intermediate principal stress σ_2 parallel to strike (Price, 1966; Sibson, 1977; Peacock et al., 2000; Peacock et al., 2016). The orientation of the fault plane is sixty degrees from horizontal and thirty degrees from σ_1. Common in extensional regimes, the Otway Basin displays numerous normal faults generated during the Cretaceous rifting of the Basin. A reverse fault is defined by movement of the hanging wall thrusting upwards relative to the footwall along the orientation of the fault plane. A reverse fault stress field is defined by σ_1 perpendicular to strike of fault, σ_2 parallel to strike and σ_3 is vertical. A strike slip fault consists of a fault plane that displaces parallel to strike of fault and in the horizontal plane (Peacock et al., 2016). A strike-slip stress field is defined by σ_1 parallel to strike of fault, σ_2 vertical and σ_3 perpendicular to strike of fault (Peacock et al., 2016). Inverted faults have been observed to have formed in the Otway Ranges, such as the Castle Cove Fault, a Cretaceous normal fault inverted during the Miocene to become a reverse fault (Figure 4).

2.6 Fractures in the Otway Ranges

Mode I fractures are extension or tensile fractures that form parallel to σ_1 (Price, 1966; Ramsay, 1980; Sibson, 1998; Laubach, 2003; Sibson, 2004; Fossen, 2010; Sage, 2013). Their direction of opening is perpendicular to σ_3 (Atkinson, 1987). Joints are the most common type of Mode I fracture and entail small magnitudes of strain, whereas fissures

are mode I fractures that are more open than joints (Atkinson, 1987). Mode I conjugate sets refer to the relationship between two intersecting fracture planes that share the equivalent stress field. The two fractures have opposite shear sense and roughly the same angle, 30° degrees from σ_1 (Atkinson, 1987). The method can be applied to compressive, extension and strike slip stress regimes. Shear fractures that display fracture parallel displacement will develop approximately 30° to orientation of σ_1. Mode II shear fractures will propagate in a sliding direction parallel to fracture and Mode III in a tearing orientation (Sibson, 1977; Atkinson, 1987; Peacock et al., 2000).

2.7 Fluid Distribution in Sedimentary Basins

Diagenesis is a significant contributor to fluid supply in sedimentary basins (Jamtveit and Yardley, 1997; Osborne and Swarbrick, June 1997). Fluid that is generated from the breakdown of solids through burial needs to be expelled and redistributed from pore space in order to not become over pressured and maintain equilibrium (Sibson, 2000). Tectonic compression, inversion and exhumation can generate rapidly fluctuating overpressures (Secor, 1965; Osborne and Swarbrick, June 1997). Pressures can rapidly increase, decrease and generate large volumes of fluid driven seismic valving and pumping through fault and fracture planes (Osborne and Swarbrick, June 1997). Positive inversion change from extension to compression over a relative short period of time and can lead to overpressures or massive fluid loss (Sibson, 2000; Sibson, 2004). Furthermore negative inversion produce overpressure reductions and can take place when stress regimes change from compression to extension forcing fluids to dilute and redistribute through extensional fracture meshes (Sibson, 1995; Sibson, 2000; Sibson, 2004).

2.8 Textures of Fracture Cements Commonly Observed

Crack-seal textures are generated through the continual Mode I reopening across a fracture with cement fill recording each increment of reopening (Laubach et al., 2010) (Laubach et al., 2004a). Crack-seal textures can display evidence of extension or compression and are common in sedimentary rocks found mostly within fault zones (Ramsay, 1980; Laubach et al., 2004a; Renard et al., 2005; Virgo et al., 2014). Cross cutting fluid cements link mechanical and cementation history of fracture fill cements (Laubach et al., 2004a). Changes in cement which have been cross-cut represent different precipitation conditions from primary to secondary fill (Laubach et al., 2004a). Calcite twinning can represent precipitation temperatures and hence burial conditions with Type I twinning generated in conditions below 200°C and Type II above (Ferrill et al., 2004).

3.0 FRACTURE MAPPING AND PETROGRAPHICAL ANALYSIS

Data was acquired through a variety of techniques. In the field, fracture orientations were measured and fracture fill recorded. Fractures were mapped to understand the rock relationship of different type of fractures. 20m x 20m transects were conducted in E-W, N-S in order to measure fractures in all orientations. Additional fracture data was obtained from a previous study (Sage, 2013). Forty-six fracture samples were collected from ten locations across the Otway Ranges (Figure 4) and petrological analysis of fracture fills was undertaken in 27 samples using the optical microscope, X – Ray mineral mapper and Scanning Electron Machine to identify fracture cement mineralogy and textures. In order to determine if fractures occurred pre or post folding, fractures were rotated relative to bedding using stereographic projection techniques. This process changes strike and dip of the original fractures and allows for analysis of pre-folding fracture sets which may have otherwise appeared to be a collection of fractures unrelated by orientation (Figure 3).

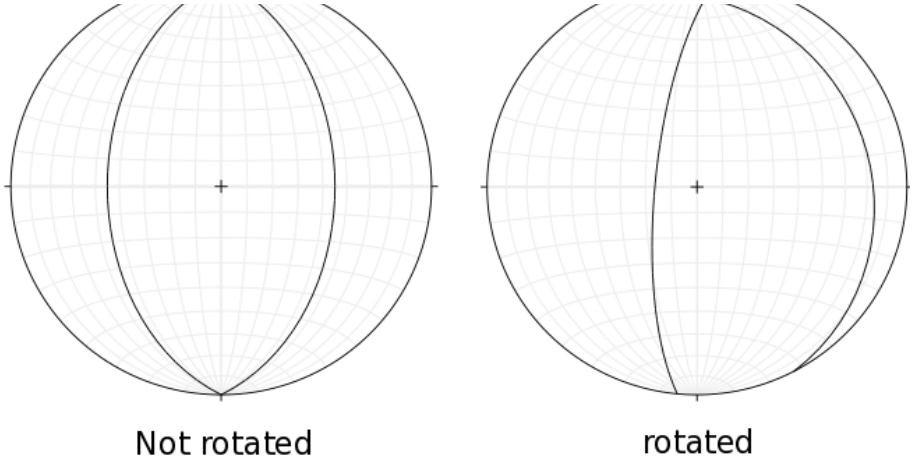

F ng) to bedding with strike of 30 degrees and dip of 20

.

4.0 FRACTURE MAPPING IN THE OTWAY RANGES

In total, 261 fracture samples were measured and recorded from 10 locations across the Otway Ranges (Figure 4). Fractures were classified based on their aperture, cement fill, dip and dip direction (Table 1). Eight fracture sets have been identified based on their orientation, stress regime, relationship relative to bedding, characteristics, cement fill and location (Table 1).

4.1 Fracture Set One

Fifty fracture planes striking in an orientation NE – SW were recorded at locations Moonlight Head, Castle Cove, Wreck Beach, Crayfish Bay and Marengo (Figure 5a). Factures dips recorded 13 fractures at 0°- 45°.Twenty-one fractures at 45°- 85° dip and 16 at 85°-90° dip. Fractures that dipped between 0°- 45° formed in a compressional stress field, 45°- 85° extensional and 85°-90° strike slip. At Moonlight Head fractures unrotated and rotated strike roughly perpendicular to bedding strike. At Castle Cove fractures unrotated and rotated strike perpendicular and parallel to bedding strike. Crayfish Bay and Marengo fractures unrotated and rotated are striking parallel to bedding strike. At Wreck Beach no bedding data was obtained. Conjugate sets were analysed at Crayfish Bay and Marengo.

Fracture Set (No. Fractures)	Location	Orientation	Nature	Conjugate Set	Cement Fill	Fracture Characteristics	Stress Regime
1 (50)	Moonlight Head, Castle Cove, Crayfish Bay, Marengo,Wreck Beach	NE-SW	Perpendicular and Parallel to bedding strike	Yes	Siderite and Calcite.	Cataclasis. Cross cut siderite and calcite.	Extension, Compression, Strike Slip
2 (26)	Castle Cove, Skenes Creek, Parker River Mouth	NNW-SSE	Parallel to bedding strike	No	Siderite and calcite	Cataclasis.	Compression and Extension
3 (8)	Castle Cove , Skenes Creek	E-W	Perpendicular to bedding strike, steeply dipping	No	Siderite.	Cataclasis.	Extension
4 (63)	Moonlight Head, Castle Cove, Crayfish Bay, Lorne Skenes Creek	NW-SE	Parallel to bedding strike. Steep and shallow dipping	Yes	Siderite and Calcite	Dominant Crack-seal and non-crack seal. Cross cut calcite	Extension or Compression
5 (59)	Castle Cove, Moonlight Head, Wreck Beach, Parker River Mouth, Cumberland River	WNW-ESE	Perpendicular to Bedding strike Vertical to steeply dipping	Yes	Siderite and Calcite	Cataclasis. Cross cut calcite	Strike Slip and Extension and compression
6 (14)	Castle Cove, Crayfish Bay, Skenes Creek	NNE-SSW	Parallel to Bedding strike. Steeply dipping	No	Siderite	Cataclasis.	Extension and Compression
7 (34)	Castle Cove	WSW- ENE	Parallel to bedding strike. Shallow and steeply dipping	Yes	Siderite and Calcite	Cataclasis, cross cut calcite	Compression or Extension
8 (7)	Castle Cove. Cumberland River	N-S	Perpendicular to bedding. Vertical and steeply dipping	No	Siderite	Not Observed	Extension

Table 1. Fracture sets interpreted from the 10 sites across the Otway Ranges.

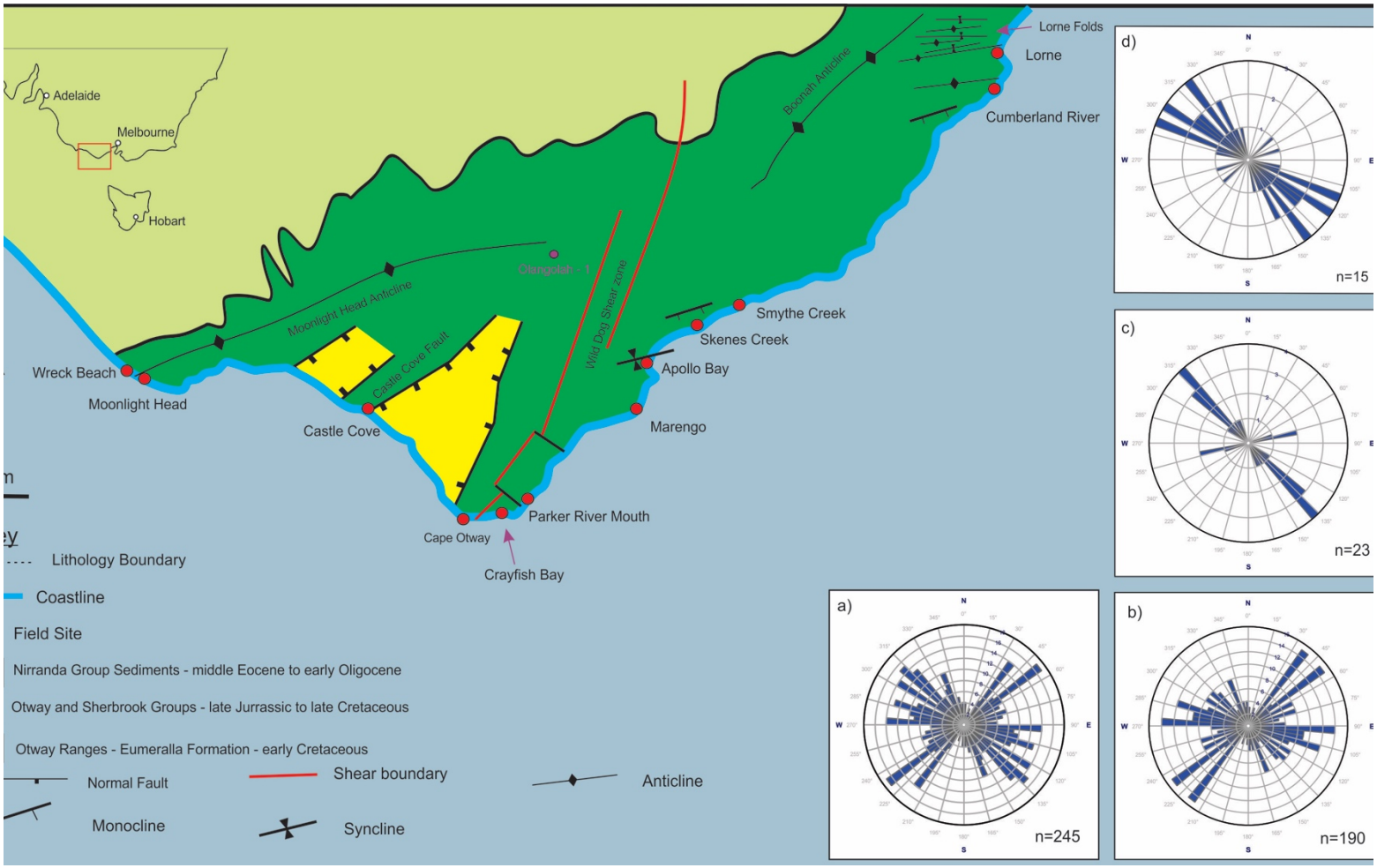

Figure 4. Field Location map of the Otway Ranges and location of Olangolah -1 well. Inset rose diagrams showing the strike of fracture planes measured. a) fracture orientation of all data b) fracture orientation of siderite only fractures c) fracture orientation of mixed fill fractures d) orientation of calcite only fractures. Structural and lithological information modified from (Duddy, 1994).

4.2 Fracture Set Two

Twenty-nine fracture planes in an orientation NNW – SSE were observed at locations Castle Cove, Skenes Creek and Parker River Mouth (Figure 5b). Eleven fractures recorded 0°- 45° dip, 17 at 45° to 85° and 1 fracture at 85°-90°. At Castle Cove unrotated fractures were striking parallel to bedding and rotated fractures 60° from bedding strike. Skenes Creek unrotated and rotated fractures were striking parallel to bedding plane. Parker River Mouth no bedding data was obtained. No conjugates were interpreted.

4.3 Fracture Set Three

At Castle Cove and Skenes Creek 8 fractures were recorded at E – W striking (Figure 5c).Two fractures recorded at 0°- 45° dip, 5 at 45°-85° and 1 at 85°-90°. At Castle Cove and Skenes Creek unrotated and rotated fractures strike perpendicular to bedding strike. No conjugate sets were analysed.

4.4 Fracture Set Four

Sixty-three fractures striking NW – SE were measured at Moonlight Head, Castle Cove, Crayfish Bay, Lorne and Skenes Creek (Figure 5d). Seventeen fractures dipped 0°-45°,43 fractures at 45°- 85° and 3 fractures at 85°-90°. Unrotated and rotated fractures at Moonlight Head, Castle Cove, Lorne, Skenes and Crayfish Bay strike perpendicular to bedding strike. Two conjugate sets were analysed at Crayfish Bay and Moonlight Head.

4.5 Fracture Set Five

Fifty-nine fractures observed WNW – ESE striking fractures were detected at Castle Cove, Moonlight Head, Wreck Beach and Parker River Mouth (Figure 5e). Twenty-one fractures dipped 0°- 45°, 23 at 45°- 85° and 10 at 85°-90°. Away from Castle Cove fault unrotated and rotated fractures strike 40° from bedding plane. At the Castle Cove Fault unrotated fractures strike perpendicular to bedding, after rotation fractures strike towards bedding plane. Moonlight head unrotated and rotated fractures strike parallel to bedding plane. A conjugate set was analysed at Castle Cove 276 N-W of the Fault.

4.6 Fracture Set Six

Fourteen NNE – SSW striking fractures were recorded at Crayfish Bay, Castle Cove and Skenes Creek (Figure 5f). Five fractures dipped 0°- 45°, 8 at 45°- 85° and 1 at 85°-90°. Unrotated and rotated fractures at Crayfish Bay strike parallel to bedding plane. At the Castle Cove fault unrotated and rotated fractures are striking oblique to bedding plane and Skenes Creek perpendicular.

4.7 Fracture Set Seven

Thirty-four fractures strike WSW – ENE only at Castle Cove (Figure 5g). 10 fractures dip at 0°- 45°, 18 at 45°- 85° and 6 at 85°-90°. Unrotated and Rotated fractures are parallel to bedding strike. A conjugate set was observed at 0°- 45°dip.

4.8 Fracture Set Eight

Seven fractures striking N-S were measured Castle Cove and Cumberland River (Figure 5h). One fracture dipping 0°- 45°, 5 at 45°- 85° and 1 at 85°-90°. Unrotated and rotated fractures at both locations strike perpendicular to bedding.

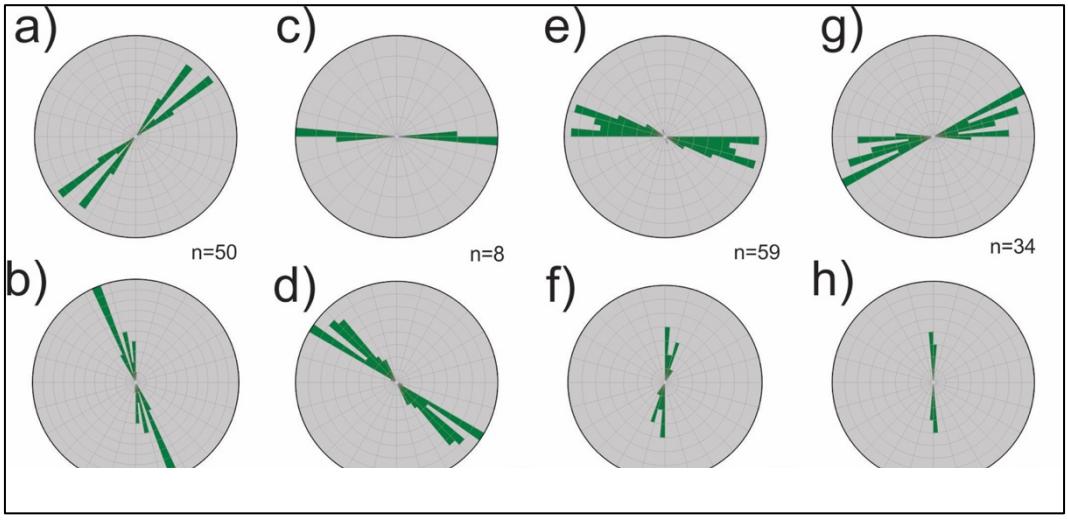

Figure 5. Rose Diagrams of all fracture sets interpreted a) Fracture Set One NE-SW b) Fracture Set Two NNW - SSE c) Fracture Set Three E-W d) Fracture Set Four NW-SE e) Fracture Set Five WNW-ESE f) Fracture Set Six NNE-SSW g) Fracture Set Seven WSW-ENE h) Fracture Set Eight N-S

5.0 PETROGRAPHY OF FRACTURE SETS IN THE OTWAY RANGES

5.1 Fracture Set One

Seventy-eight percent of fractures are filled by siderite or goethite (weathered product of siderite) cement, 2% calcite and 6% cataclastic deformation with siderite cement (Figure 6). Fourteen percent had no fill. Sampled from Castle Cove, Wreck Beach and Marengo. Minerals constrained within the walls of the fracture consist of goethite and an iron, titanium baring aluminosilcate. Rounded quartz grains are found within samples that display cataclastic deformation and angular grains of host rock can be seen within fractures than have undergone infill brecciation (Figure 6a). Goethite has a mineral association with aluminosilicate and are generally found together along with albite and plagioclase. A fracture containing an orthoclase fluid cement deviates from the trend of past work that the only fluids within the Otway Basin are siderite and calcite (Figure 6g). The host rock of Fracture Set One samples adjacent to the fracture cements consist of albite, quartz, plagioclase, orthoclase and Fe, Ti aluminosilicate (Figure 6).

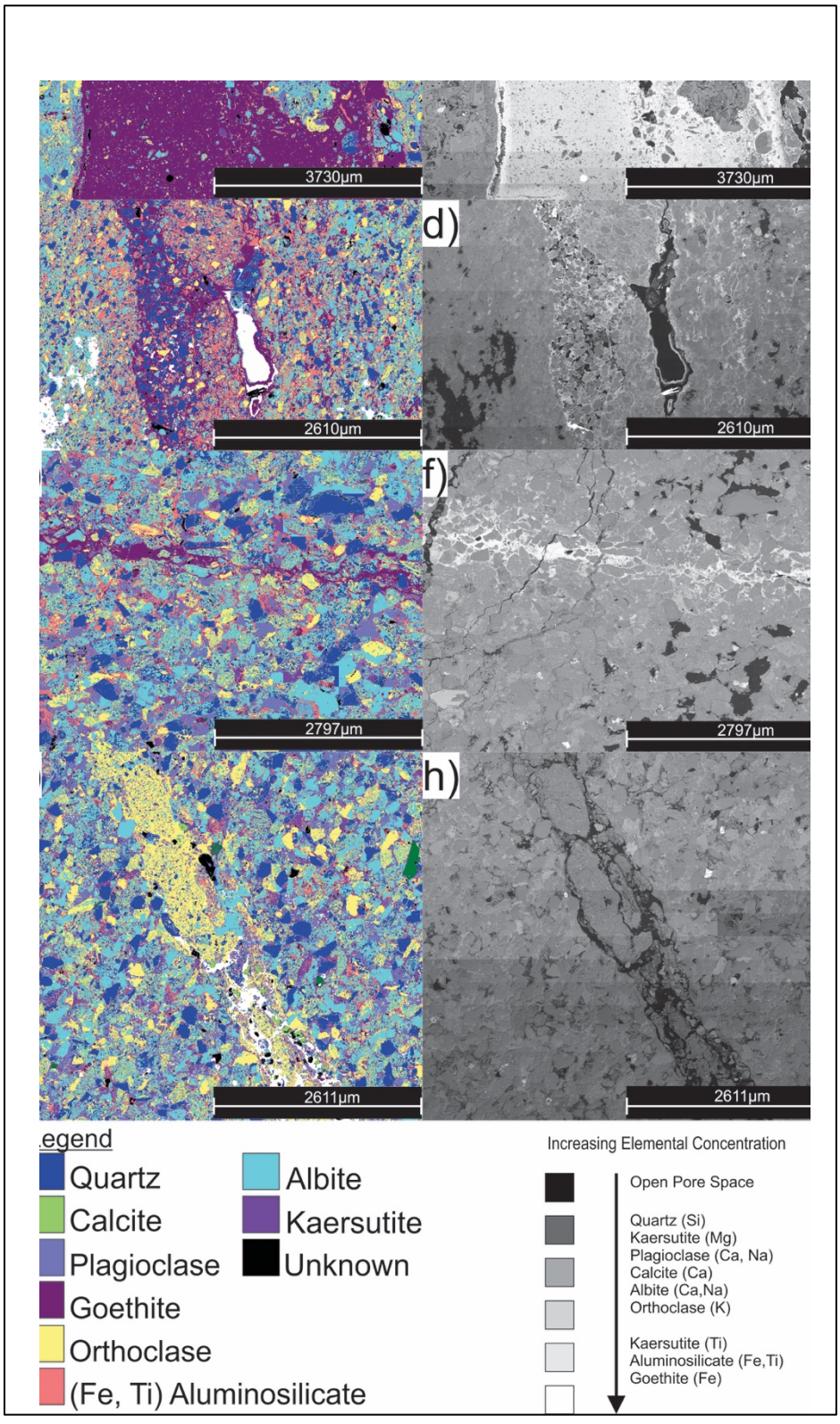

Figure 6. Fracture Set 1 a), b) X-Ray mineral map and Back-Scatter Electron (BSE) image of Wreck Beach (LFWB04) siderite fracture c), d) X-Ray mineral map and BSE of Castle Cove (LFCC02) siderite fracture) e), f) X-Ray mineral map and BSE of Marengo siderite fracture (LFM01) g) X-ray mineral map and h) BSE of Crayfish Bay orthoclase fracture LFCB02.

5.2 Fracture Set Two

Thirty-eight percent of fractures are cemented with siderite fill, 10% with calcite and 11% display siderite cemented cataclasis. Forty-one percent contained no fill. No crack seal texture was observed in any of the samples. Sampled from Skenes Creek (Figure 7). The fracture cements consist of goethite and Fe, Ti baring aluminosilicate. The goethite and aluminosilicate are both located discretely within the fracture and fracture walls (Figure 7). Fractures appear to represent a dilation plane of siderite within discrete pore openings of the rock, then a clear tensile failure of the host rock itself (Figure 7). The host rock surrounding the fractures consist of extensive albitisation of plagioclase and orthoclase. Quartz is present along with small percentages of kaesutite.

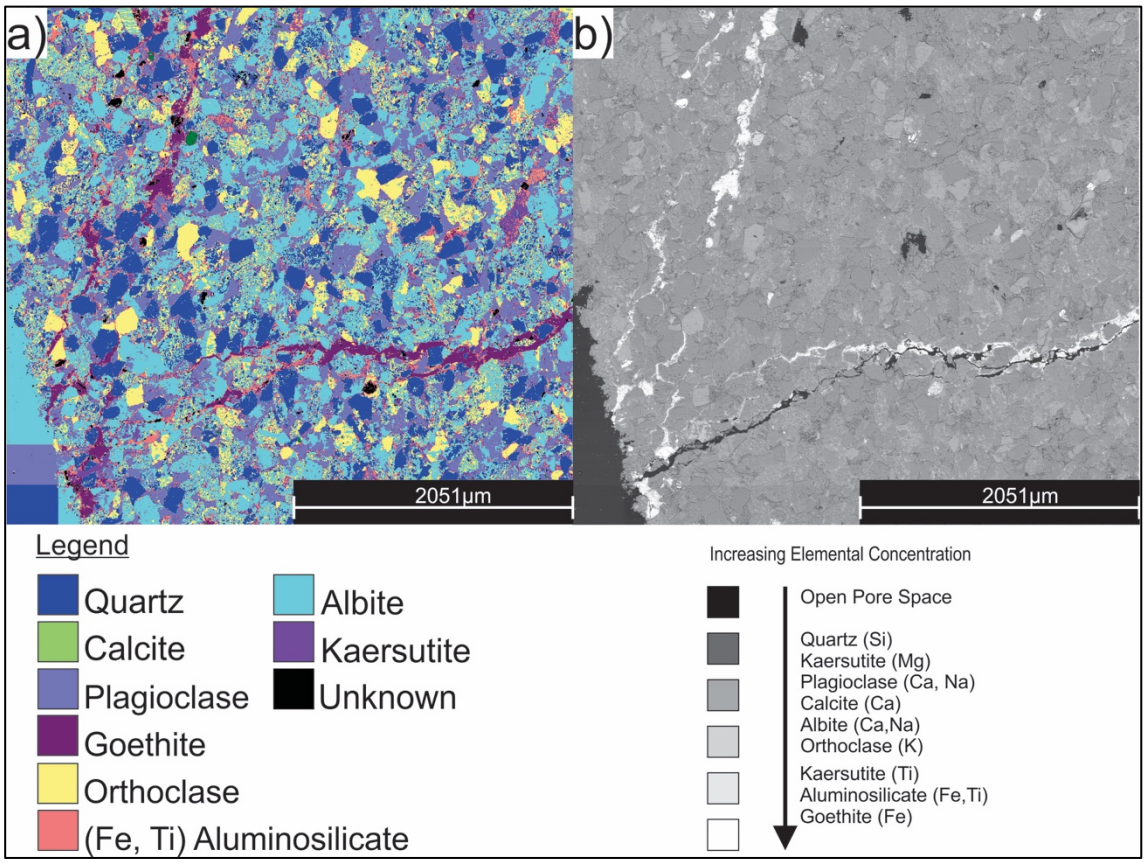

Figure 7. Fracture Set 2 a) X-Ray mineral map of two siderite fractures from Skenes Creek (LFSK04) b) BSE image of Skenes Creek sample (LFSK04).

5.3 Fracture Set Three

No fractures contain calcite cement with only one fracture experiencing cataclastic deformation containing siderite cement. Sampled from the Castle Cove Fault. Optical petrology displays extensive fracturing of quartz grains. Siderite infiltration of pore space was displayed within host rock, further albitisation of orthoclase and plagioclase was observed

5.4 Fracture Set Four

Fourty-six percent of fractures contain siderite cement and 23% calcite cement. One sample displayed cataclastic deformation with siderite cement. Twenty-eight percent of fractures contain no fill. Sampled from Castle Cove, Moonlight Head, Lorne and Skenes Creek. Thirty-three percent of the calcite fracture cements displayed crack – seal kinematics in samples from Moonlight Head and Lorne. Multiple phases of calcite cements are displayed with some samples showing up to four phases of Mode I rupturing and subsequent calcite fluid intrusion and cementation (Figure 11).
Cross cutting calcite through siderite is observed in 33% of samples and Type I twinning of calcite crystals within samples from Lorne is prominent (Figure 11c). Castle Cove calcite fracture cements provide evidence of extensive deformation of calcite crystals with subsequent re-entering of siderite fluid. Samples from all locations contained significant percentages of albite in the host rock as a result of diagenesis of plagioclase, orthoclase and Fe-Ti aluminosilicate is apparent (Figure 8).

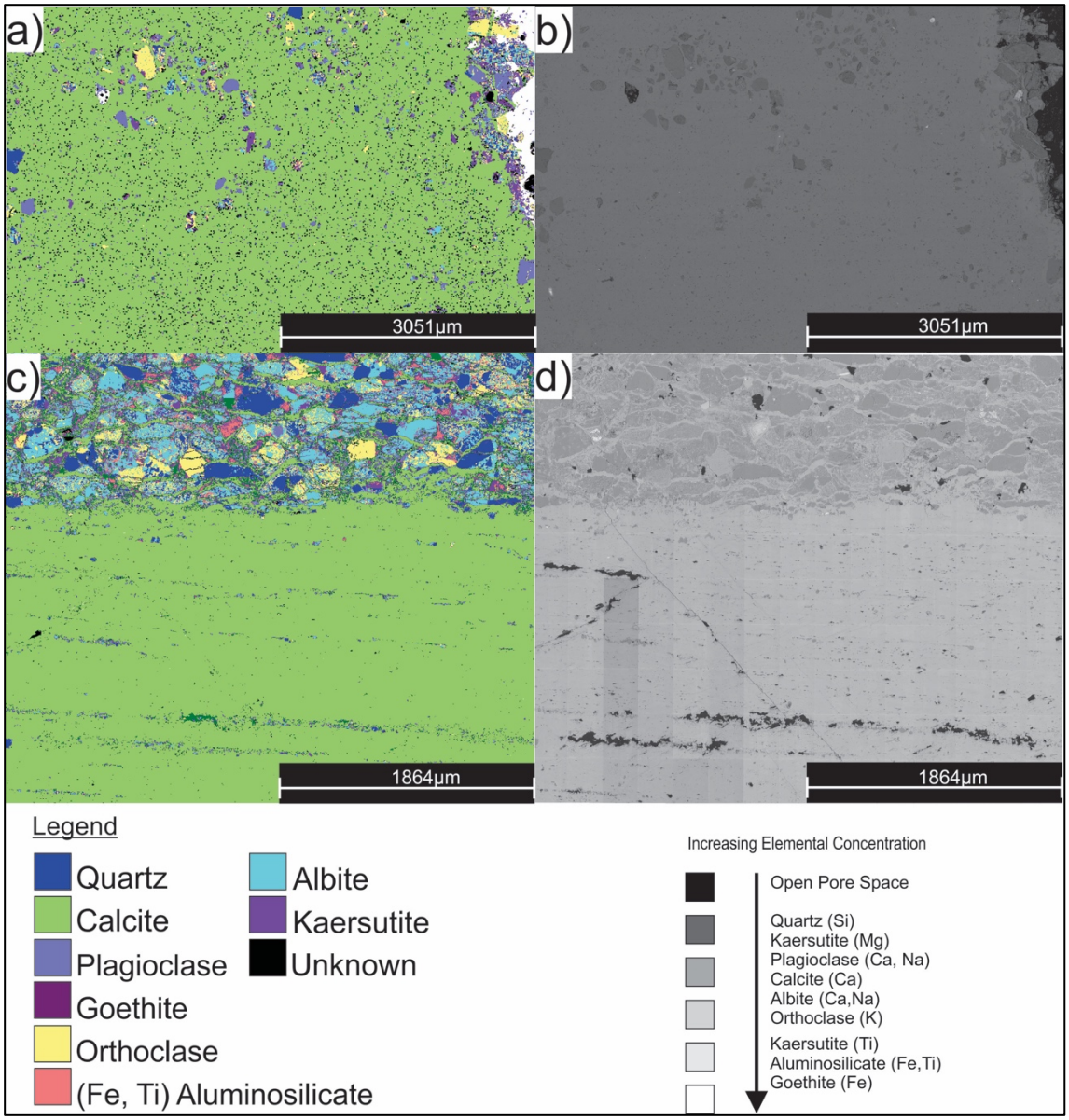

Figure 8. Fracture set 4 a) X-Ray mineral map of Moonlight Head calcite fracture (LFMH02) b) BSE image of Moonlight Head calcite fracture. c) X-Ray mineral map of Lorne calcite fracture (LFL02) d) BSE image of Lorne calcite fracture (LFL02).

5.5 Fracture Set Five

Eighty-six percent of fracture cements contain siderite, 8% calcite cements and 5% cataclastic deformation with siderite cement. One percent of fractures contained no fill. Sampled from Castle Cove, Cumberland River, Wreck Beach, Parker River Mouth and Lorne. Castle Cove displayed evidence of cataclastic deformation of quartz grains with siderite cement infiltrating the fracture (Figure 9a). No samples displayed calcite crack

– seal textures. Seventy-five percent of the calcite cements were observed cross cutting through siderite (Figure 9c). At Parker River Mouth siderite is cross cut by calcite (Figure 9c). Cumberland River displayed calcite cross cutting a siderite fracture (Figure 9e and Figure 11d). Wreck Beach samples containing calcite also cross-cut siderite cement. Fe, Ti baring aluminosilicate is present directly surrounding the fracture in close proximity to siderite. Albite and other minerals remain consistent within the host rock along with high percentages of quartz and orthoclase (Figure 9).

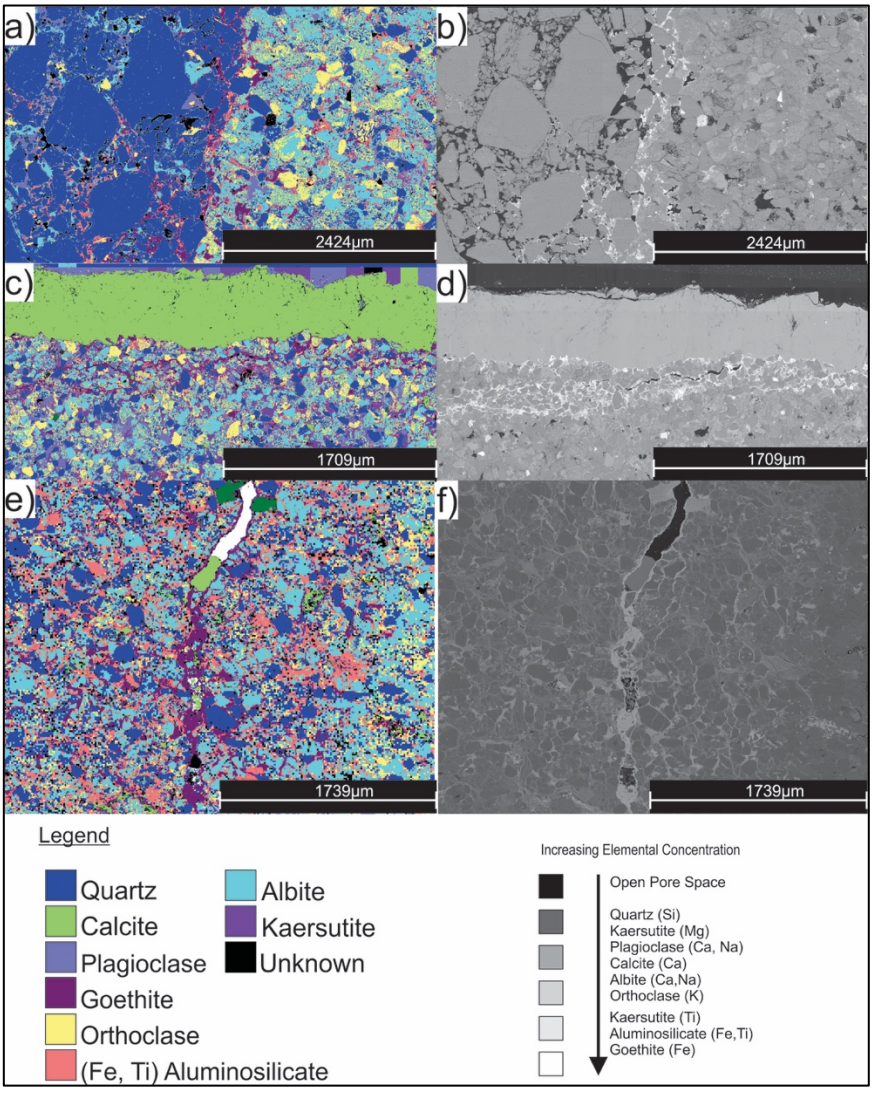

Figure 9. Fracture Set 5 a) X-Ray mineral map of Castle Cove siderite fracture (LFCC04) b) BSE image of Castle Cove siderite fracture (LFCC04) c) X-Ray scatter mineral map of Parker River Mouth (LFPM02) calcite and siderite fracture d) BSE image of Parker River Mouth (LFPM02) calcite and siderite fracture e) X-ray mineral map Cumberland River (CR01) f) BSE of Cumberland River (CR01)

5.6 Facture Set Six

Fifty-seven percent of fracture cements contain siderite, no calcite cements were observed and 21% of fractures displayed cataclastic deformation with siderite cement most notable at the Caste Cove Fault. Twenty-two percent of fractures contained no fill. Sampled from Skenes Creek, Crayfish Bay and Castle Cove. Diagenesis of host rock was consistent, with orthoclase and plagioclase transitioning into albite. No observations using the X-Ray mineral mapper and BSE were utilised with samples in Fracture Set Six.

5.7 Fracture Set Seven

Seventy-nine percent of fracture cements contained siderite. Three percent contained calcite and 3% cataclasitc deformation with siderite cement. Fractures taken 276m NW of the castle Cove Fault display three phases of fluid flow. Calcite cross cutting original flow of siderite and along with kaersutite cross cutting the calcite (Figure 11c). The fracture itself is cross cut by another calcite fracture striking NE-SW (Fracture Set One) (Figure 10a). Type I twinning of calcite crystals is also displayed within the fracture (Figure 11f). Host rock adjacent to fracture is dominated by albite, plagioclase, orthoclase and Fe-Ti bearing aluminosilicate.

5.8 Fracture Set Eight

No samples were analysed from Fracture Set Eight.

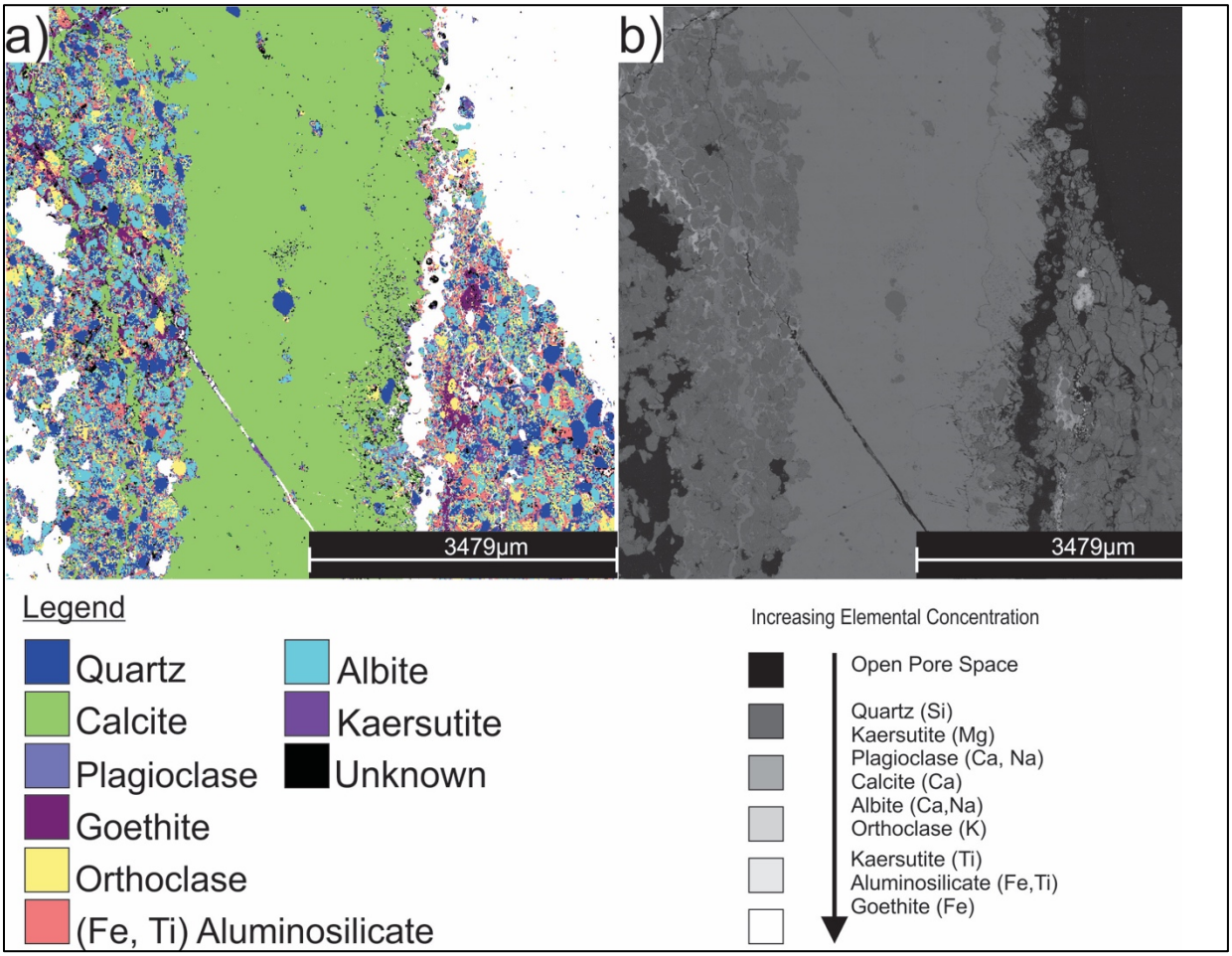

Figure 10. Fracture Set 7 a) X – Ray mineral Map of Castle Cove calcite and siderite fracture (LFCC1902) b) BSE image of Castle Cove calcite and siderite fracture (LFCC02).

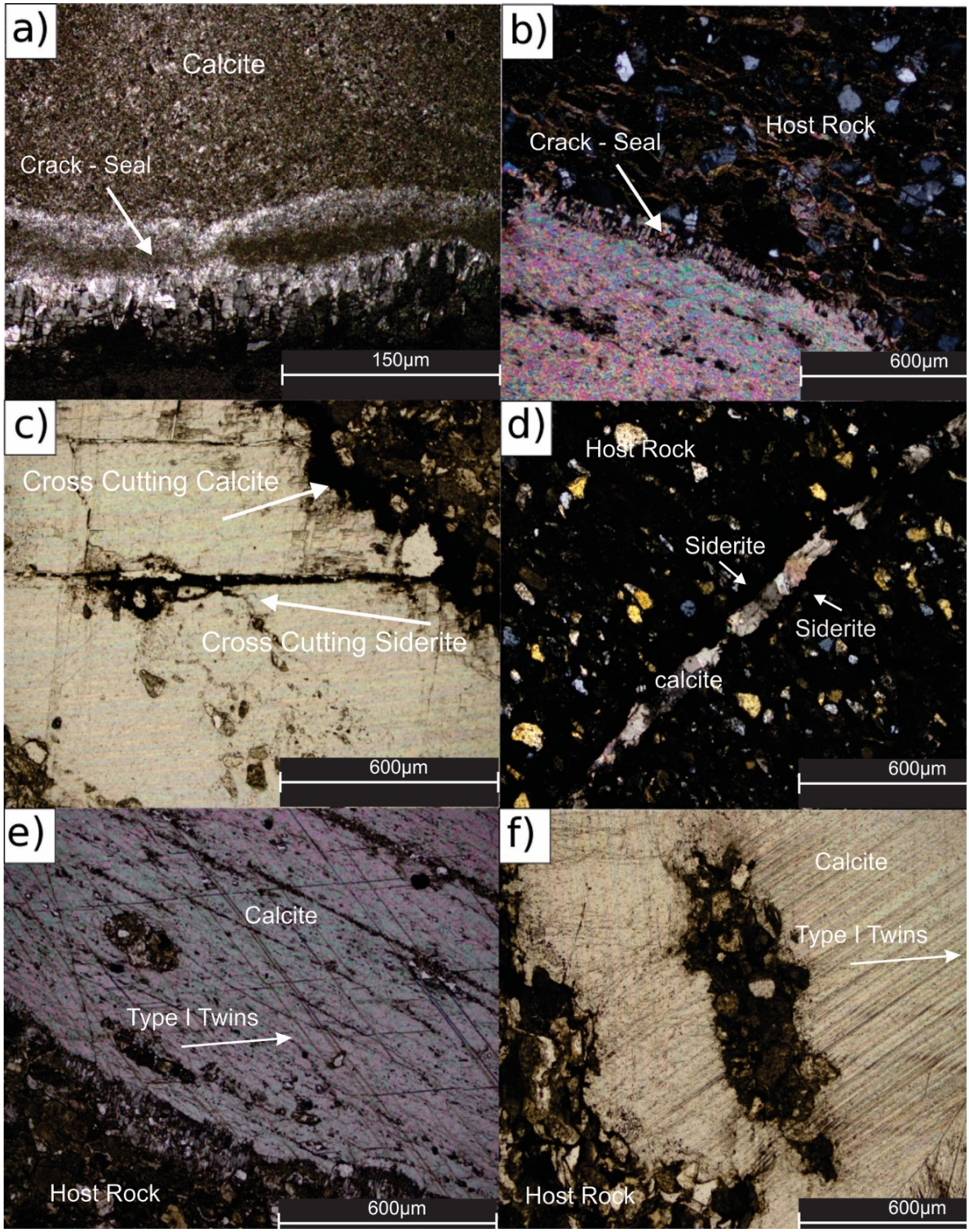

Figure 11. a) Plane polarised light Moonlight Head (LFMH02) sample representing four crack seal phases b) Cross polarised Lorne (LFL02) sample representing two calcite fill phases c) Plane polarised Castle Cove cross cutting feature (LFCC1902) d) Cross polarised Cumberland River (CR01) sample with calcite cross cutting siderite e) Cross polarised Lorne calcite fracture sample with Type I twinning (LFL02) f) Plane polarise Castle Cove calcite and siderite fracture with Type I twinning (LFCC1902).

6.0 Deformation Bands at Castle Cove

The Castle Cove Fault displayed fractures representing discrete bands of deformation from Fracture Sets 1, 2, 3, 5, 6 and 7 (Table 1) (Figure 12). A deformation band is defined by a low displacement deformation surface (Rawling and Goodwin, 2003; Fossen and Bale, 2007; Fossen et al., 2007). Sampled from within the damage zone of the Castle Cove Fault, fracture orientations varied significantly with dips from shallow to steep. Many samples represented compaction bands, a type of deformation band where the grain size of the band is larger than host rock (Figure 12a). The deformation bands represent areas where siderite has infiltrated the pore space created by the fracturing of grains.

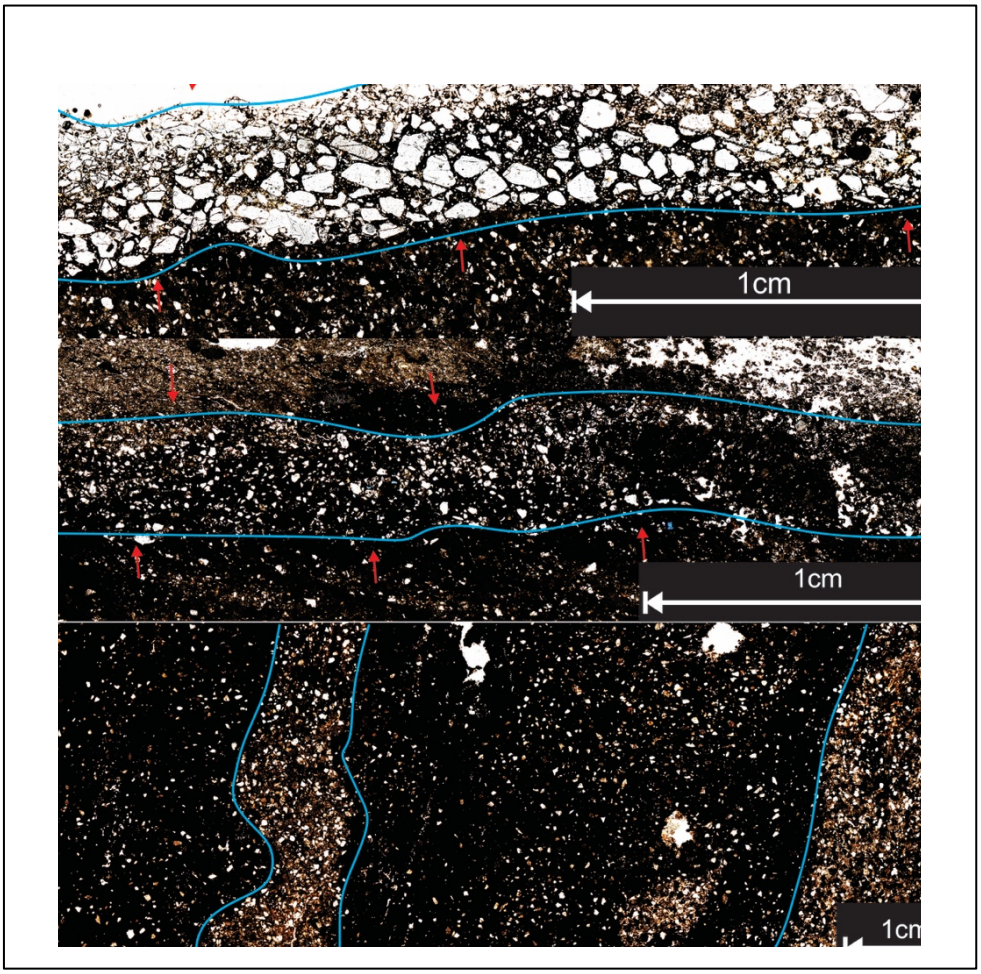

Figure 12. Castle Cove Deformation bands. Blue line represents area of band. a) Plane polarised light (PPL) siderite deformation band (LFCC04) b) PPL siderite deformation band LFCC02 c) PPL siderite deformation band (CC05 from Sage, 2014).

7. 0 DISCUSSION

7.1 RELATIONSHIP OF FRACTURES TO LARGE SCALE STRUCTURES IN THE OTWAY RANGES

Large scale geological structures, such anticlines and faults, are a result of deformation of the lithosphere. Fractures are more likely to be parallel with faults, tensile fractures will generate on the limbs of anticlines and shear fractures will generate on the axial trace of an anticline (Gillespie et al., 1993). If fractures are also a direct representation of deformation and the two share a relationship, then fractures can be associated with large scale structures (Savage and Brodsky, 2011; Eckert et al., 2014).

7.2 Fractures connected to Moonlight Head Anticline

The Moonlight Head Anticline runs NE- SW through the Otway Ranges (Figure 4). The uplift of the Moonlight Head Anticline is discussed to have limited association with the mid – Cretaceous exhumation event (Duddy, 2002; Duddy, 2003). It is claimed the exhumation of Moonlight Head is related to Miocene NW – SE compression of the Otway Ranges (Figure 2). Evidence from Vitrinite Reflectance (VR) and Apatite Fission Tract Analysis (AFTA) show that uncomformably sitting Eocene sediments overlying Cretaceous Otway Group sediments both share the same VR and AFTA values (Duddy, 2002; Duddy, 2003). The VR values imply that burial temperatures were likely post – Eocene, which puts the exhumation of Moonlight Head likely around the Miocene (Duddy, 2002; Duddy, 2003). Fracture Set Four recorded at Moonlight Head strikes NW – SE and displays Mode I opening perpendicular at NE – SW orientation (Figure 13). Based on borehole breakouts which give the orientation of the least horizontal stress across the Otway Basin, σ_h is orientated at roughly NNE – WSW (Hillis et al., 1995). Coupled with Miocene to contemporary NW - SE directions of maximum principal stress, it can be argued Fracture Set Four was generated not

during the mid-Cretaceous exhumation but the Neogene post Oligocene exhumation events in the Otway Ranges (Perincek et al., 1994; Duddy, 1997; Sage, 2013; Holford et al., 2014).

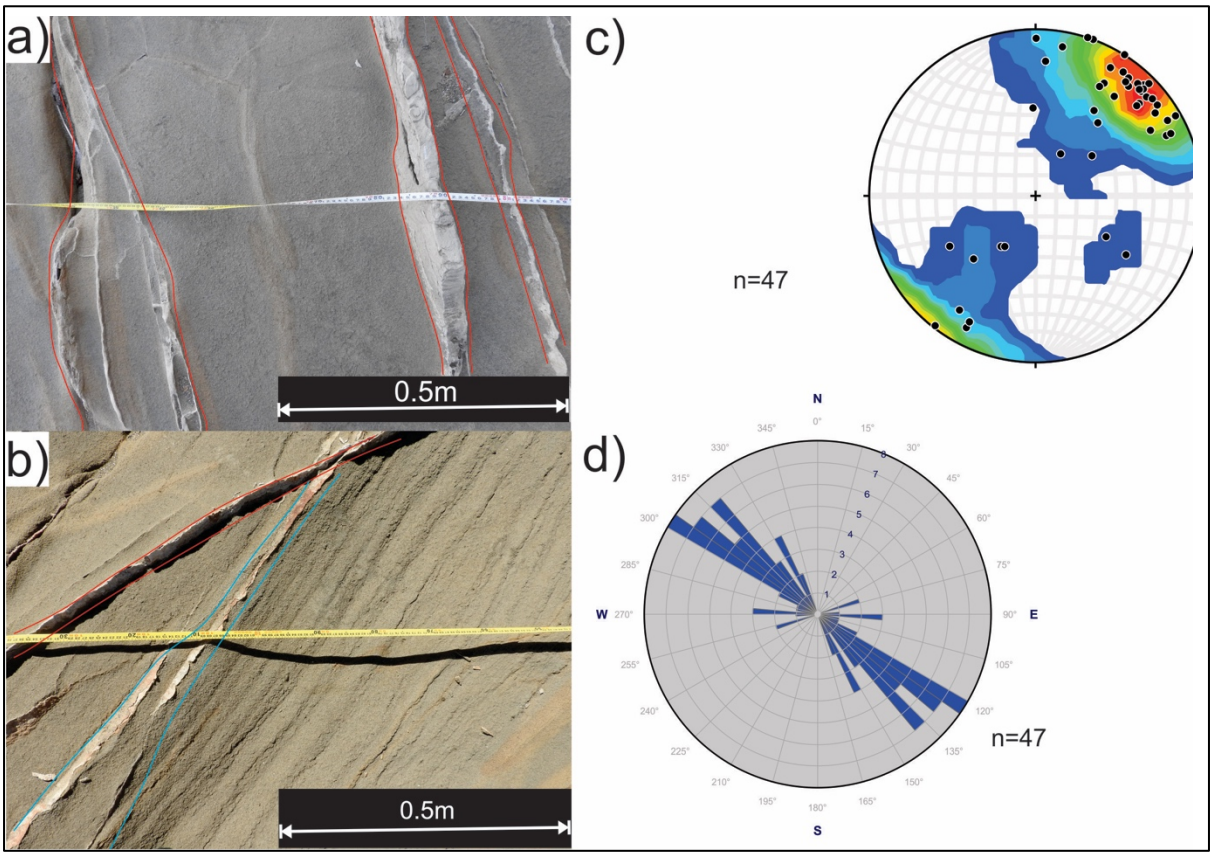

Figure 13. a) and b) Sample calcite fractures observed and collected during structural transect in the field at Moonlight Head. Red and Blue indicates areas of fractures c) Contour stereonet of poles to planes of unrotated Fracture Set Four at Moonlight Head d) Rose Diagram of Fracture Set Four recorded at Moonlight Head.

7.3 Fractures related to Wild Dog Shear zone

The Wild Dog Shear Zone (WSZ) strikes roughly NNE – SSW and is related to a lower – Cretaceous transfer fault from the rifting of Australia and Antarctica (Duddy, 1994). The Wild Dog Shear zone cuts through the Otway Ranges roughly in-between Cape Otway and Crayfish Bay (Figure 4). Cape Otway is situated west of the Shear Zone and Crayfish Bay, east. Fractures recorded by (Sage, 2013) and data collected at Crayfish Bay displayed Fracture Set One with steeply dipping NE-SW fractures close to parallel with the shear zone (Sage, 2013). Cape Otway displays dominant NNW – SSE striking fractures (Fracture Set Two) not seen at Crayfish Bay along with a minor NNE – SSW (Fracture Set Six) trending

set (Sage, 2013). Crayfish Bay and Cape Otway are situated only a few hundred metres apart but share distinctively different deformation and burial histories. Established VR evidence from Cape Otway demonstrated that the area experienced burial temperatures of 350°C, inferring that the western side of the Wild Dog Shear Zone must have experienced massive up-lift and erosion of approximately 6km, implying the dominant Fracture Set Two of NNW – SSE striking fractures occurred during the mid-Cretaceous rapid exhumation event (Duddy, 1994; Duddy, 2002). Crayfish Bay on the eastern side of the Wild Dog Shear Zone has VR data inferring significantly less burial temperatures115°C and depths, coupled with a significantly less dominant Fracture Set Two and Fracture Set Four (Duddy, 2002; Sage, 2013). Compared to Cape Otway, it implies the dominant NE- SW Fracture Set One at Crayfish Bay was generated in the process of mid – Cretaceous exhumation but at shallower depths than at Cape Otway and maybe more associated with the movement of the Wild Dog Shear Zone itself (Figure 14) (Duddy, 2002).

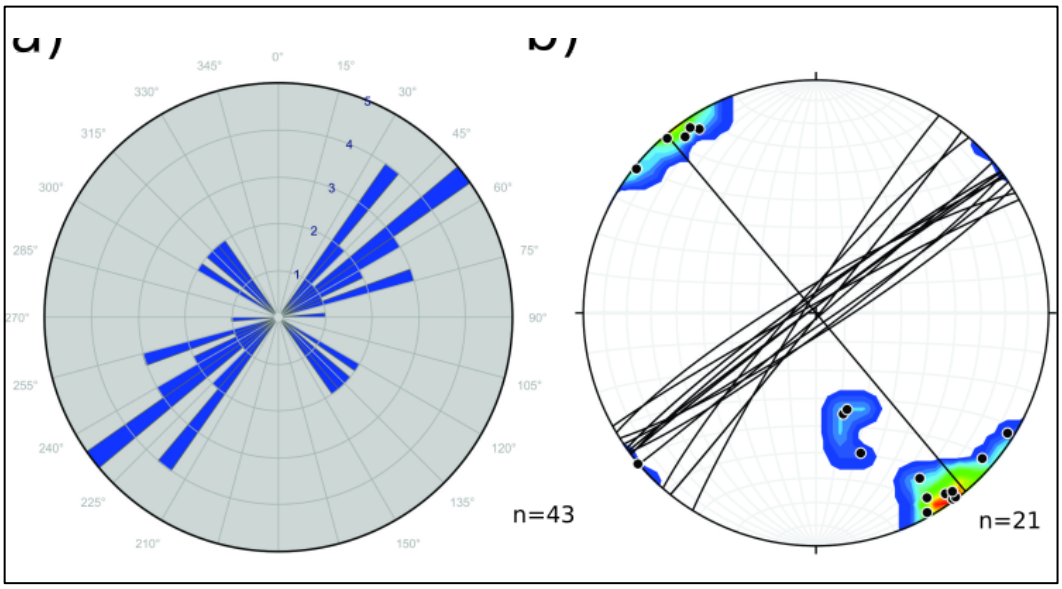

Figure 14. a) Rose diagram of Fracture Set One (NE – SW) and Fracture Set Four (NW – SE) measured during Crayfish Bay transect b) Contour stereonet of Fracture Set One measured at Crayfish Bay, displaying planes and poles to planes.

7.4 Fractures related to Castle Cove

The Castle Cove Fault is a mid-Cretaceous normal fault inverted in the Neogene to become a reverse fault, striking NE – SW (Figure 15a) (Holford et al., 2011b). This can be confirmed with the observation of folded Eocene sediments on top of the structure in the hanging wall indicating the inversion must have taken place post Eocene (Sage, 2013). The Castle Cove Fault allows the observation of the interaction of fractures close to the fault and away from the fault. Beginning with the interpretation of fractures adjacent to the fault a dominant NE – SW Fracture Set One can be observed and argued to be directly related to the initial fault activation or the Miocene reactivation due to the similar nature in strike (Figure 15b) (Sage, 2013). Vitrinite Reflectance analysis conducted of the Narrawaturk Marl (Nirranda Group Sediment) on top of the fault implies burial conditions related to the Miocene exhumation event rather than the mid – Cretaceous event (Duddy, 2002). A second set of NE – SW trending fractures (Fracture Set One) is observed to have been created before folding and reactivation due to their different strikes relative to NE – SW when rotated. Furthermore, a large proportion of other fracture sets measured at the fault are roughly perpendicular to bedding. This is argued by (Tassone, 2014) to have placed the fractures forming prior to reactivation or folding of the Castle Cove Fault.

Fractures measured 276m NW of the Castle Cove Fault displayed Fracture Set One NE - SW, Fracture Set Five WNW – ESE striking almost perpendicular to bedding plane and Fracture Set Four striking parallel to bedding strike at NW – SE (Figure 15d). Rotating fractures towards bedding had a limited effect on the orientation of fractures and can thus be interpreted the fractures formed prior to Miocene folding and or after reactivation of the fault and subsequent folding. Further evidence from VR and AFTA at Castle Cove provides temperatures of >100°C inferring burial conditions and fractures are closely related to the

lower-Cretaceous extension and mid – Cretaceous exhumation events (Duddy, 1994; Duddy, 2002). It can therefore be interpreted that Fracture Set One, Fracture Set Five and Fracture Set Four away from the faults are most likely related to Cretaceous tectonic events rather than Miocene events.

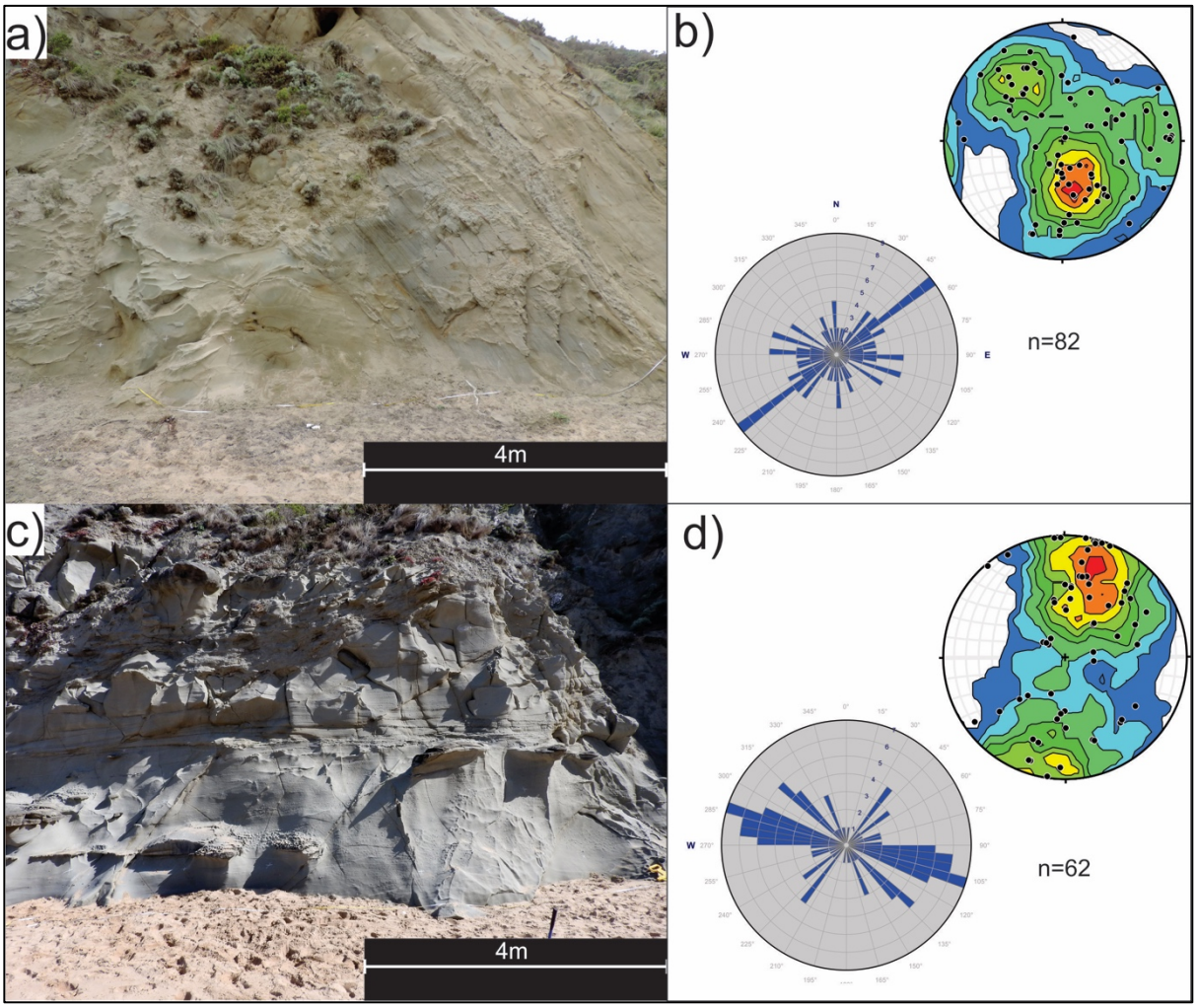

Figure 15. a) Sample and measurement location of fractures at the Castle Cove fault b) Rose diagram of unrotated dominant Fracture Set One (NE-SW) strike and contour stereonet of poles to planes of all fracture measurements recorded at the fault c) Sample and measurement location of fractures 276 NW of the Castle Cove Fault d) Rose diagram of unrotated fracture strikes displaying Fracture Set One (NE – SW) Fracture Set Four (NW – SE) and Fracture Set Five (WNW – ESE) and contour stereonet of poles to planes of measurements recorded away from the Castle Cove fault.

8.0 RELATIONSHIP OF FRACTURE SETS TO LARGE SCALE FLUID FLOW

Fluid history is complex in the Otway Ranges due to similar overprinting events involving the mid – Cretaceous burial and exhumation events coupled with the Oligocene, Miocene burial and exhumation events (House et al., 2002; Holford et al., 2011b). It is however still

possible to relatively confine fluid flow history to the deformational history of the Otway Ranges (Sibson, 1995).

8.1 Fluid Flow Associated with Fracture Set one

As explained in section 5.1, siderite cements are common and calcite cements rare in Fracture Set One. Multiple phases of fluid flow can be interpreted, through linking deformation events with individual locations. Wreck Beach fracture cements exhibited multiple pulses of siderite cement episodes, each containing difference concentration of iron (Figure 6b). Marengo displayed a single phase siderite fracture, representing more of a dilational shear plane and lacking recognisable fracture walls due to deformation of grains (Figure 6e). At Crayfish Bay Fracture Set One samples display a single event orthoclase fluid cement (Figure 6g). The Castle Cove Fault cements display intensive cataclastic deformation and reactivation of fractures containing siderite (Figure 6c). Timing of fluid at Wreck Beach can be associated with two deformation events. Based on the orientation and steepness of dip, NW – SE extension or strike – slip during lower -Cretaceous rifting. It could additionally be a result of reactivation as based on VR, Wreck Beach received extensive deformation and uplift during the Miocene (Duddy, 2002). The multiple phases of siderite cement indicate possible seismic hydraulic valving through positive inversion which can involve massive fluid discharge when a system goes from an extensional to compressional regimes (Sibson, 2000; Osborne and Swarbrick, June 1997). The orthoclase fracture cement at Crayfish Bay is abnormal and not seen in other samples collected across the Otway Ranges nor discussed in any literature. It implies the idea that Crayfish Bay experienced a deeper burial regime with higher temperatures to melt the orthoclase. This is contentious with evidence from (Duddy, 1994; House et al., 2002) that Crayfish Bay only experienced temperatures of 120°C during lower -Cretaceous burial . At Marengo the sample observed strikes parallel to bedding very steeply

at almost 90° and is part of the dominant fracture set recorded at Marengo by (Sage, 2013). Fluid flow at Marengo can only be associated to one deformation event related to the Cretaceous rifting and burial due to its steep dip, its characteristic of a shear plane and VR values implying Cretaceous burial (Duddy et al., 1994). Siderite fluid flow at the Castle Cove Fault (Figure 4) can be constrained to two deformation events. AFTA and VR data values constrain the fault to mid – Cretaceous which is likely the time when siderite fluid first entered the system (Duddy, 1994). Samples at the fault display catacalstic deformation with siderite cements implying reactivation and inflow of siderite that could have conceivably occurred during the Miocene inversion of the fault (Dewhurst and Jones, 2002).

8.2 Fluid Flow Associated with Fracture Set Two

Two episodes of siderite and calcite fluid flow can be interpreted with evidence from Skenes Creek. Fluid flow at Skenes Creek can be linked to two deformation events from the lower – Cretaceous to Miocene which represent times in which fluid may have entered the system. The Skenes Creek Monocline (Figure 4) is implied to be a result of a Cretaceous fault reactivated during the Miocene (Duddy, 1994). A separate scenario implies initial mid-Cretaceous deformation from uplift based on evidence from AFTA and VR. They display temperatures of 240°C for the heavily folded mid-Cretaceous section adjacent to the Monocline (Duddy, 1994; Tassone, 2014).

8.3 Fluid Flow Associated with Fracture Set Three

One fracture sample from Fracture Set Three has a fluid cement. This fracture is a cataclastic siderite band from the Castle Cove Fault. With two deformation events discussed in section 7.3 at the Castle Cove Fault this fracture is also likely related to the two events during lower – Cretaceous faulting and Miocene inversion. A lack of representative data for Fracture Set Three makes it difficult to make any definitive conclusions.

8.4 Fluid Flow Associated with Fracture Set Four

Fracture cements in Fracture Set Four exhibited the strongest evidence for fracture reactivation observed from calcite cement crack seal textures and cross cutting fracture cements. With 46% of fractures containing siderite and 23% containing calcite the most of any fracture set, Fracture Set Four has strong indications of multiple episodes of fluid flow. Calcite samples from Moonlight Head showed Mode I fractures with multiple punctuated reactivation crack – seal events. Mode I fractures are useful as they display the orientation of maximum principal stress (Figure 12a) (Sibson, 1977). Calcite cements at Moonlight Head and Wreck Beach were observed to cross cut siderite fractures. This relatively time constrains siderite to before calcite fill, with the siderite providing zones of weakness, increasing the likelihood for reactivation and subsequent calcite flow (Becker et al., 2010). At Lorne there is additional evidence of multiple phases of fluid flow with calcite cements observed to cross cut siderite cements with the addition of crack-seal textures. Three phases of fluid flow away from the Castle Cove Fault can be observed with calcite fractures cements exhibiting crystals that were heavily deformed and cross cut with siderite cements. Deformation events that can explain the timing of fluid flow at Moonlight Head has been explained in section 7.2, especially in regards to Fracture Set Four with calcite fill likely related to Miocene exhumation at Moonlight Head and Wreck Beach. At Lorne timing of fluid can be implied to have occurred during one deformation event involving the NE trending Lorne Syncline and Boonah Anticline which are both linked to Miocene NW – SE compression (Perincek.D and C.D, 1995; Holford et al., 2011a; Holford et al., 2011b; Holford et al., 2014; Tassone, 2014). Generation of fluid flow away from the Castle Cove fault can be linked to Cretaceous deformation which is explained in section 7.4 for Fracture Set Four.

8.5 Fluid Flow Associated with Fracture Set Five

Two episodes of fluid flow are observed in Fracture Set Five with 86% of fracture cements displayed are siderite and 8% calcite. At Parker River Mouth calcite is observed to cross cut siderite (Figure 9c). At Cumberland River calcite is also observed to cross cut siderite (Figure 9e) Timing of fluid generation is difficult to constrain but can be implied from maximum palaeotemperatures at Parker River Mouth and Cumberland River that place them during mid – Cretaceous burial and exhumation (Duddy, 1994). Limited evidence is implied for Miocene compression related fluid timing.

8.6 Fluid Flow Associated with Fracture Set Six

Only two episodes of siderite fluid flow can be implied for Fracture Set Six with all fractures only containing the single cement. Sampled from Castle Cove, Crayfish Bay and Skenes Creek (Table 2). The timing of fluid flow is linked to the deformation events which are explained earlier for Castle Cove, Crayfish Bay and Skenes Creek to be likely Cretaceous or Miocene in age.

8.7 Fluid Flow Associated with Fracture Set Seven

Three episodes of fluid flow are observed. With evidence away from the Castle Cove Fault. A calcite fracture cement cross cuts siderite cement which then cross cuts calcite cement. The fluid can be linked to deformation away from the fault which is explained in section 7.4 to be during Cretaceous deformation. Siderite cements at the fault as explained earlier are likely timed with the deformational events associated with the fault.

8.8 Fluid Flow Associated with Fracture Set Eight

No Fracture cements were observed in Fracture Set Eight.

9.0 FLUID FLOW TIMING IN THE OTWAY RANGES

9.1 Calcite Fractures

Calcite is only apparent in Mode I open fractures. (English, 2012) discusses the likelihood of Mode I fracture formation during tectonic environments due to thermal contraction as a result of rapid cooling from subsidence and subsequent rapid compressional uplift. Pore pressure of lithology is also important with Mode I fractures probable when uplift occurs in over-pressured and tectonically quiescent environments (English, 2012). The tectonic history of the Otway Ranges fits this model with two events of thermal contraction, during the NW - SE inversion period of the mid – Cretaceous rapid cooling event and during NW - SE inversion during the Miocene. (Becker et al., 2010) and (Laubach et al., 2004a) discuss that tensile crack – seal mechanics are likely to form in sandstones that are significantly buried due to the incremental forcing nature of compressional tectonics along with thermo-elastic effects. Crack seal textures with calcite fluid were prominent in Fracture Set 4 at Moonlight Head and Lorne which were constrained to Miocene inversion. Furthermore, a large proportion of Fracture Set Four calcite cements were non-crack seal. A significantly less percentage of calcite fracture cements were part of Fracture Set One, Fracture Set Two, Fracture Set Five and Fracture Set Seven. This implies evidence that these specific fractures did not have to be optimally aligned for NW-SE compression to allow calcite fluid flow, making it more difficult to constrain the specific timing of fluid flow (Laubach et al., 2004b). This is due to the orientations of Fracture Set One and Seven that can be implied to be associated in times of extension during lower Cretaceous rifting and upper Cretaceous to Oligocene rifting. However, the pattern observed is that predominately calcite fractures are NW – SE striking (Fracture Set Four) and appear in Mode I fractures (Figure 4d). This constrains calcite cement fill to compressional events in the Otway Ranges as Mode I fractures strike parallel to the orientation of maximum horizontal stress (Twiss and M.Moores, 2007). It can consequently

be argued that calcite fluid flow initiated during the mid-Cretaceous or created and perhaps reactivated during Miocene inversion (Figure 16).

9.2 Siderite Fractures

Pervasive siderite is apparent in Fracture Sets One to Seven identified, regardless of mode type, dip angle, strike and orientation to bedding (Figure 4b). Siderite appeared immediately after burial, filling pore space as result of diagenesis of volcanogenic detritus consisting of an (Fe – Ti) baring aluminiosilicate (Duddy, 2003). Based on this explanation siderite would have been present in fractures created during initial extensional deformation and burial during the lower-Cretaceous of the Otway Basin. Mobilisation of siderite would be repeated for all major tectonic periods of deformation that create new fluid pathways through either shearing of grains or tensile mechanics. Based on this argument siderite fluid is present from initial lower Cretaceous burial to at least Miocene inversion and compression (Figure 16). It can be further debated that siderite is still locked up in pore spaces deeply buried and therefore any future tectonic deformation events may produce siderite fluid cements.

9.3 Mixed Fracture Cements

All fractures that are mixed with siderite and calcite strike commonly as part of Fracture Set Four however this characteristic is also apparent in Fracture Sets One, Two, Five and Seven (Figure 4c) (Figure 5d) (Figure 16). The calcite cross cuts the siderite in almost all cases which indicates siderite must have come before the calcite, perhaps during the initial burial of the Eumeralla Formation during the lower – Cretaceous (Figure 2). The calcite cement would have entered later during times of NW – SE compression like the mid – Cretaceous and Miocene inversion as mixed fracture cements are characterised by Mode I stresses which explains why mixed fracture sets still predominately strike in favour of Fracture Set Four (Figure 16).

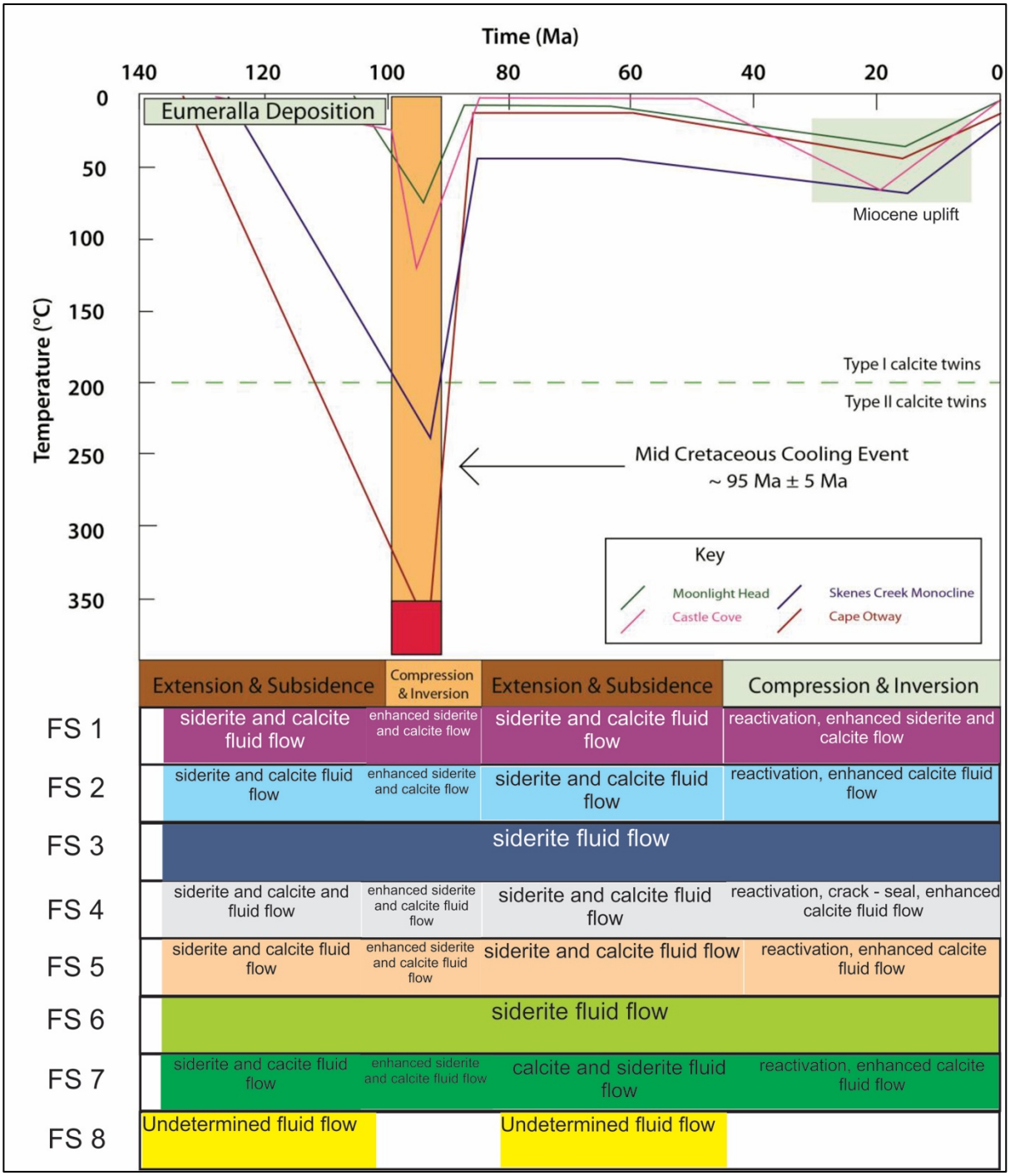

Figure 16. Thermal History, Time (Ma) versus Temperature (°C) plot calculated from vitrinite reflectance (VR) values and apatite fission tract analysis (AFTA) displaying Mid – Cretaceous rapid burial and cooling along with Miocene cooling events for locations in the Otway Ranges (Duddy, 1994; Sage, 2013).Associated times of tectonic deformation are included along with temperatures of Type I and Type II twinning (Ferrill et al., 2004). Interpreted timing of fracture sets (FS) and fluid flow are displayed corresponding to times of deformation.

10.0 IMPLICATIONS OF STRUCTURAL PERMEABILITY ACROSS THE OTWAY RANGES

The Otway Basin has seen extensive compaction from burial and diagenesis of grains that has significantly reduced overall effective porosity and permeability in the region (Duddy, 2003; Tassone, 2014). The Eumeralla has seen porosities calculated at Moonlight Head and Cape Otway to be 7.15% and 0.36%. The number of fractures open at surface and fractures that were once open but are currently cemented preventing fluid flow displays a good proxy of structural permeability and hence prospective permeability networks of the Otway Ranges. Research conducted by (Tassone, 2014) and (Laubach et al., 2010) discuss that cemented fractures acts as planes of weakness and can be favourably reactivated given the right environment (Figure 17). Based on this the Otway Ranges can be inferred to have favourable conditions for enhanced fluid pathways considering the number of cemented fractures observed purely in outcrop at the surface. Evidence interpreted in discussion argues for this statement explaining that Fracture Set Four in the Otway Ranges are the best representations of fractures to have undergone reactivation during mid – Cretaceous inversion and the Miocene compression resulting in enhanced fluid flow. Siderite cement is observed acting as potential planes of weaknesses with numerous fractures cross cut by calcite cement. Additionally, calcite cements in Fracture Set Four also display evidence of cement weakness with numerous observations of reactivation with crack seal textures. It also needs to be considered that fracture cements can make a fracture, stress insensitive rendering the fractures closed to reactivation and fluid flow (Laubach et al., 2004a; Laubach et al., 2004b). The type of cementation is important depending on whether the fracture is cemented by clay smear or cohesionless cataclasis (Dewhurst et al., 2002).

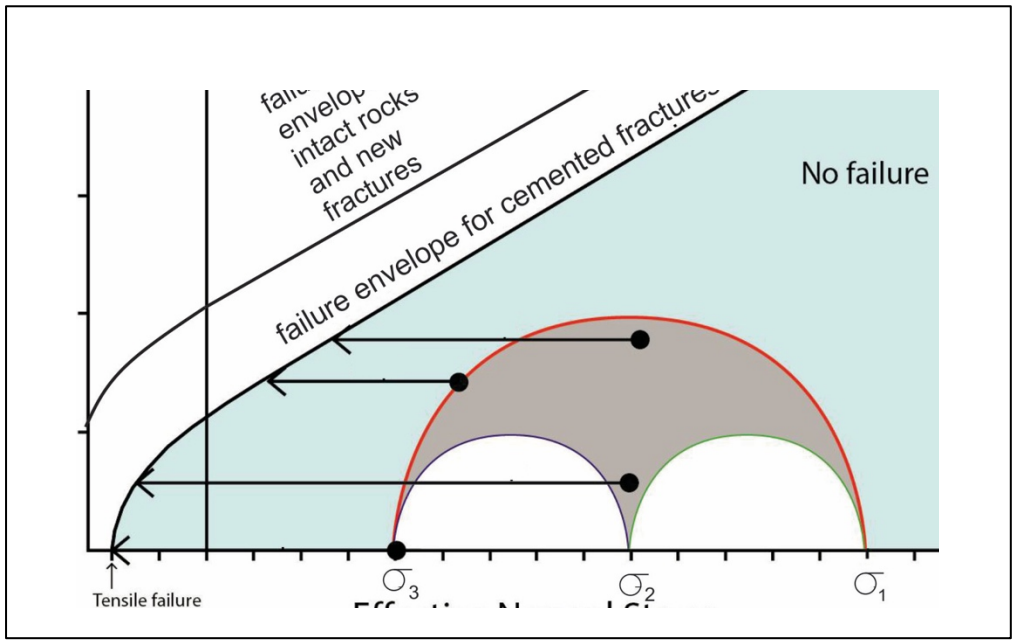

Figure 17. Mohr Circle schematic showing failure envelope of cemented fracture and intact rocks. A change in stress or increase in pore pressure will push circle to lower failure envelope first (Sage, 2013) (Dewhurst et al., 2002).

These characteristics may make the fracture cement stronger than the host rock lithology, increasing the likelihood of fracture reactivation to be promoted into the host rock sediments rather than the fracture cement itself (Dewhurst and Jones, 2002; Dewhurst et al., 2002). Fracture susceptibility plots by (Tassone, 2014) display fracture susceptibility based on a strike slip fault stress regime in the Otway Basin (Figure 18). Fracture Set Two, Fracture Set Four, Fracture Set Five and Fracture Set Eight when modelled in a strike slip fault regime are the most susceptible to reactivation opening perpendicular to σ_H (Figure 18b,d,e,h). Fractures orientated in these directions provide enhanced fluid pathways for hydraulic reactivation of fractures. It must be noted however that evidence has shown that this does not prevent fluid from entering other fractures that are not optimally aligned for reactivation, with multiple episodes of fluid flow observed in Fracture Sets One and Fracture Set Seven (Figure 18a,18g).

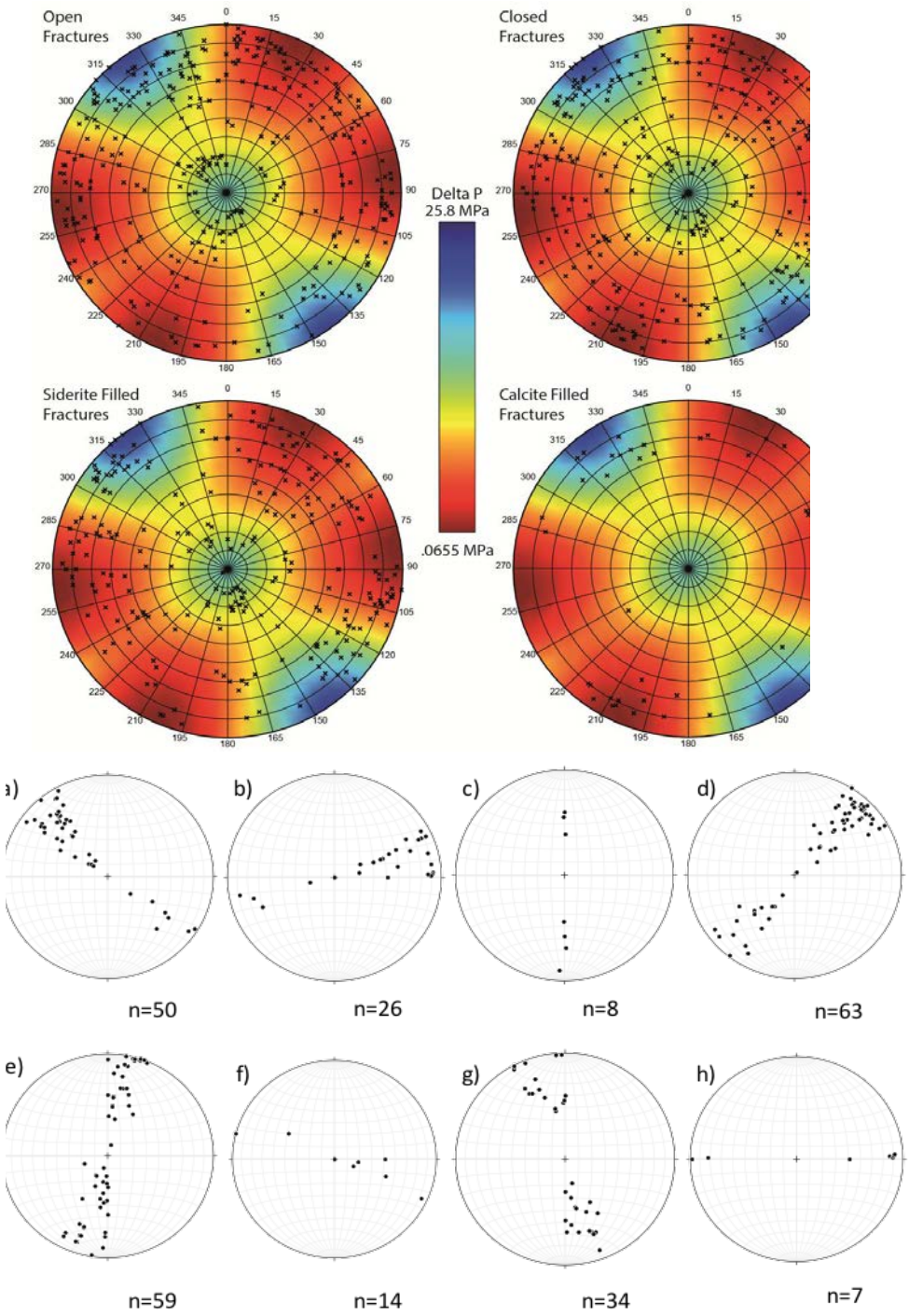

Figure 18. Fracture susceptibility plots from for the Otway Basin at 1km depth in a strike-slip fault regime (Tassone, 2014) plotted against a) Fracture Set One b) Fracture Set Two c) Fracture Set Three d) Fracture Set Four e) Fracture Set Five f) Fracture Set Six g) Fracture Set Seven h) Fracture Set Eight. Delta P values represent pore pressure increases in (MPa) required to generate brittle failure in the rock. Blue values represent values which are furthest from failure and red values represent orientations and dips of fractures closest to failure. They require the least amount of pore pressure for reactivation. These values can also signify likelihood of new fracture and faults to form. Poles to fracture planes represent fracture values corresponding to fracture type in each fracture susceptibility plot title.

11.0 CONCLUSIONS

1. Two-hundred-sixty-one fractures were measured across the Otway Ranges from ten separate locations exclusively from the Eumeralla Formation (Otway Group). In total 27 thin sections were used for petrographic analysis. The petrological study of all thin section samples was conducted using an optical microscope and SEM interpreting fracture cements and kinematics.

2. Eight Fracture Sets were identified with defined orientations, different locations, cement fills, cement textures and associated stress regimes.

3. Petrography off all fracture sets identified displayed host rock of extensive albite, goethite (weathered siderite), volcanogenic aluminosilicate, orthoclase, plagioclase and quartz. Internal fracture minerals consisted of goethite but are indicated as siderite due to goethite being the weathered product of siderite. Steeply dipping siderite fractures mostly from Castle Cove displayed dominant cataclastic deformation of grains while calcite fractures often displayed Type I Twinning, Mode I characteristics, crack – seal textures and cross cut siderite.

4. Timing of Fracture Set Four at Moonlight Head were interpreted to be likely Miocene in age. Fracture Set One at Crayfish Bay was constrained to lower, mid- Cretaceous extension and exhumation. Fracture Sets One, Four and Five at Castle Cove to be lower –Cretaceous extension, burial and possibly reactivation during exhumation in the Miocene inversion and compression.

5. Multiple episodes of enhanced calcite fluid flow in Fracture Set One, Fracture Set Two, Fracture Set Four and Fracture Set Five can be confidently constrained to times of NW- SE compression during mid Cretaceous exhumation and Miocene compression. These fractures sets also imply to a lesser extent fluid flow during times of extension in the Otway Basin.

6. Siderite fluid flow in the Otway Ranges was constrained to Fracture Sets One, Fracture Set Two, Fracture Set Three, Fracture Set Four, Fracture Set Five, Fracture Set Six and Fracture Set Seven. These fractures propose generation and timing of fluid flow was during all deformation events from lower Cretaceous burial to Miocene compression and inversion.

7. Fracture susceptibility models by (Tassone, 2014) suggest steeply dipping calcite and siderite fractures as part of Fracture Set Two, Fracture Set Four, Fracture Set Five and Fracture Set Eight are likely to reactivate with Fracture Set Four displaying the most evidence for reactivation. Fracture Sets One, Fracture Set Three, Fracture Set Six and Fracture Set Seven are the least likely to reactivate.

RECOMMENDATIONS

Further studies can be conducted in order to better constrain the origin and timing of fluid flow in the Otway Basin. Methods such as oxygen and carbon isotope geochemistry of the fracture cements can help constrain more precise burial temperatures and hence if the fluids were related to mid-Cretaceous exhumation or Miocene compression and inversion (Bons et al., 2012). Radiogenic Sr isotopes studies conducted on calcite cements can also provide an age of the fracture cements. Cathodoluminescence is a good method to identify crack – seal mechanics and timing of fluid flow (Laubach et al., 2004a). Well preserved samples are required however in order to achieve this.

ACKNOWLEDGMENTS

I'd like to thank all the people who have guided me throughout the perilous journey of creating an honours thesis. Firstly, many thanks to my supervisor, Dr. Rosalind King for directing me towards the correct path during each increment of my thesis, who knows where my project would have ended up. My co – supervisor, Dr. Simon Holford for his rapid reply to emails regarding literature material along with his continual support throughout the year. I'd like to notably thank PhD student Natalie Debenham for her help with field work and assisting me with structural data interpretation. I'd also like to thank Dr. Rowan Hansberry for his support along with his experience during field work and thin section preparation. Aoife Mcfadden from Adelaide Microscopy for scrupulously helping me with the Scanning Electron Machine. Continental Instruments for cutting roughly forty thin sections and sending them halfway across the world, intact. ARC Discovery Project for financial support and finally, the Honours 2016 cohort for always making those long days manageable by providing quality banter.

REFERENCES

ATKINSON B. K. 1987. Fracture mechanics of rock. Fracture mechanics of rock. Academic Press,

BAILEY A., KING R., HOLFORD S., SAGE J., BACKE G. & HAND M. 2014. Remote sensing of subsurface fractures in the Otway Basin, South Australia. *Journal of Geophysical Research: Solid Earth* **119**, 6591-6612.

BECKER S. P., EICHHUBL P., LAUBACH S. E., REED R. M., LANDER R. H., BODNAR R. J. & BECKER R. J. 2010. A 48 m.y. history of fracture opening, temperature, and uid pressure: Cretaceous Travis Peak Formation, East Texas basin. *Bulletin of the Geological Society of America* **122**, 1081-1093.

BONS P. D., ELBURG M. A. & GOMEZ-RIVAS E. 2012. A review of the formation of tectonic veins and their microstructures. *Journal of Structural Geology* **43**, 33-62.

BRIGUGLIO D., HALL M. & KEETLEY J. 2015. Structural evolution of the Early Cretaceous depocentres, Otway Basin, Victoria. *Australian Journal of Earth Sciences*, 1-17.

DEWHURST D. N. & JONES R. M. 2002. Geomechanical, microstructural, and petrophysical evolution in experimentally reactivated cataclasites applications to fault seal prediction. *AAPG Bulletin* **86**, 1383-1405.

DEWHURST D. N., JONES R. M., HILLIS R. R. & MILDREN S. D. 2002. Microstructural and Geochemical Characterisation of Fault Rocks from the Carnarvon and Otway Basins. *APPEA Journal* **42** 167 - 186

DUDDY I. 1997. Focussing exploration in the Otway Basin: Understanding timing of Source Rock maturation. *APPEA Journal*.

DUDDY I. R. 1994. The Otway Basin: Thermal, Structural, Tectonic and Hydrocarbon Generation Histories. *Australian Geological Survey*, 35-42

DUDDY I. R., GREEN P. F., BRAY R. J. & HEGARTY K. A. 1994. Recognition of the thermal effects of fluid flow in sedimentary basins. *Geological Society of London* **78**, 325-345.

DUDDY I. R. 2002. The Otway Basin: Geology, Sedimentology, Diagenesis AFTA (c) Thermal Histroy Reconstruction and Hydrocarbon Prospectivity (National Centre for Petroleum Geology and Geophysics, Adelaide) Geotrack International Pty. Ltd, Brunswick West Victoria

DUDDY I. R. 2003. Mesozoic: a time of change in tectonic regime. *Geological Society of Australia Special Publication* **23**.

ECKERT A., LIU X. & CONNOLLY P. 2014. Large-scale mechanical buckle fold development and the initiation of tensile fractures. *Geochemistry, Geophysics, Geosystems* **15**, 4570-4587.

ENGLISH J. M. 2012. Thermomechanical origin of regional fracture systems. *AAPG Bulletin* **96**, 1597-1625.

FERRILL D. A., MORRIS A. P., EVANS M. A., BURKHARD M., GROSHONG JR R. H. & ONASCH C. M. 2004. Calcite twin morphology: a low-temperature deformation geothermometer. *Journal of Structural Geology* **26**, 1521-1529.

FOSSEN H. & BALE A. 2007. Deformation bands and their influence on fluid flow. *AAPG Bulletin* **91**, 1685-1700.

FOSSEN H., SCHULTZ R. A., SHIPTON Z. K. & MAIR K. 2007. Deformation bands in sandstone: a review.(Research Article). *Journal of the Geological Society* **164**, p. 755.

FOSSEN H. 2010. Structural Geology. Structural Geology. Cambridge University Press,

GILLESPIE P. A., HOWARD C. B., WALSH J. J. & WATTERSON J. 1993. Measurement and characterisation of spatial distributions of fractures. *Tectonophysics* **226**, 113-141.

HILL K. A., COOPER G. T., RICHARDSON M. J. & LAVIN C. J. 1994. Structural Framework of the Eastern Otway Basin: Inversion and Interaction Between Two Major Structural Provinces. *Exploration Geophysics* **25**, 79-87.

HILL K. A., FINLAYSON D. M., HILL K. C. & COOPER G. T. 1995. Mesozoic tectonics of the Otway Basin region: the legacy of Gondwana and the active Pacific margin - a review and ongoing research. *APPEA Journal* **35**, 467-493.

HILLIS R. R., MONTE S. A. & TAN C. P. 1995. The contemporary stress field of the Otway Basin, South Australia: Implications for hydrocarbon exploration and production. *APPEA Journal* **35**, 494-506.

HOLFORD S., HILLIS R., DUDDY I., GREEN P., STOKER M., TUITT A., BACKÉ G., TASSONE D. & MACDONALD J. 2011a. Cenozoic post-breakup compressional deformation and exhumation of the southern Australian margin. *APPEA Journal* **51**, 613-638.

HOLFORD S. P., HILLIS R. R., DUDDY I. R., GREEN P. F., TASSONE D. R. & STOKER M. S. 2011b. Paleothermal and seismic constraints on late Miocene–Pliocene uplift and deformation in the Torquay sub-basin, southern Australian margin. *Australian Journal of Earth Sciences* **58**, 543-562.

HOLFORD S. P., TUITT A. K., HILLIS R. R., GREEN P. F., STOKER M. S., DUDDY I. R., SANDIFORD M. & TASSONE D. R. 2014. Cenozoic deformation in the Otway Basin, southern Australian margin: implications for the origin and nature of post-breakup compression at rifted margins. *Basin Research* **26**, 10-37.

HOUSE M. A., KOHN B. P., FARLEY K. A. & RAZA A. 2002. Evaluating thermal history models for the Otway Basin, southeastern Australia, using (U-Th)/He and fission-track data from borehole apatites. *Tectonophysics* **349**, 277-295.

JAMTVEIT B. & YARDLEY B. 1997. Fluid Flow and Transport in Rocks: Mechanisms and Effects. Fluid Flow and Transport in Rocks: Mechanisms and Effects. Chapman and Hall,

KRASSAY A., CATHRO D. & RYAN D. 2004 A regional tectonostratigraphic framework for the Otway Basin. Eastern Australasian Basins Symposium II, Petroleum Exploration Society of Australia, Special Publication. pp. 97-116.

LAUBACH, REED R. M., OLSON J. E., LANDER R. H. & BONNELL L. M. 2004a. Coevolution of crack-seal texture and fracture porosity in sedimentary rocks: cathodoluminescence observations of regional fractures. *Journal of Structural Geology* **26**, 967-982.

LAUBACH, EICHHUBL P., HILGERS C. & LANDER R. H. 2010. Structural diagenesis. *Journal of Structural Geology* **32**, 1866-1872.

LAUBACH S. E. 2003. Practical approaches to identifying sealed and open fractures. *AAPG Bulletin* **87**, 561-579.

LAUBACH S. E., OLSON J. E. & GALE J. F. W. 2004b. Are open fractures necessarily aligned with maximum horizontal stress? *Earth and Planetary Science Letters* **222**, 191-195.

LYON P. J., BOULT P. J., HILLIS R. R. & BIERBRAUER K. 2007. Basement controls on fault development in the Penola Trough, Otway Basin, and implications for fault-bounded hydrocarbon traps. *Australian Journal of Earth Sciences* **54**, 675-689.

MILLER J. M., NORVICK M. S. & WILSON C. J. L. 2002. Basement controls on rifting and the associated formation of ocean transform faults—Cretaceous continental extension of the southern margin of Australia. *Tectonophysics* **359**, 131-155.

OSBORNE M. J. & SWARBRICK R. E. June 1997. Mechanisms for Generating Overpressure in Sedimentary Basins: A Reevaluation. *AAPG Bulletin* **81**, 1023-1041.

PEACOCK D. C. P., KNIPE R. J. & SANDERSON D. J. 2000. Glossary of normal faults. *Journal of Structural Geology* **22**, 291-305.

PEACOCK D. C. P., NIXON C. W., ROTEVATN A., SANDERSON D. J. & ZULUAGA L. F. 2016. Glossary of fault and other fracture networks. *Journal of Structural Geology*.

PERINCEK D., COCKSHELL C. D., M.FINLAYSON D. & HILL K. A. 1994. The Otway Basin: Early Cretaceous rifiting to Miocene strike-slip. *Australian Geological Survey* 27-33.

PERINCEK.D & C.D C. 1995. The Otway Basin: Early Cretaceous Rifting to Neogene Inversion. *APPEA Journal* **35**, 451-466.

PRICE N. J. 1966. Fault and joint development in brittle and semi-brittle rock. Fault and joint development in brittle and semi-brittle rock. Pergamon Press, [1st ed.] ed.

RAMSAY J. G. 1980. The crack-seal mechanism of rock deformation. *Nature* **284**, 135-139.

RAWLING G. C. & GOODWIN L. B. 2003. Cataclasis and particulate flow in faulted, poorly lithified sediments. *Journal of Structural Geology* **25**, 317-331.

RENARD F., ANDREANI M., BOULLIER A.-M. & LABAUME P. 2005. Crack-Seal Patterns: Records of Uncorrelated stress release variations in crustal rocks. *Geological Society of London* **243**, 67-69.

SAGE J. M. 2013 Fault and Fracture Networks in the Otway Basin, Victoria; Implications for Structural Permeability. Earth Sciences. pp. 1-117. The University of Adelaide.

SAVAGE H. M. & BRODSKY E. E. 2011. Collateral damage: Evolution with displacement of fracture distribution and secondary fault strands in fault damage zones. *Journal of Geophysical Research: Solid Earth* **116**, n/a-n/a.

SECOR D. T., JR. 1965. Role of fluid pressure in jointing. *American Journal of Science* **263**, 633-646.

SIBSON R. H. 1977. Fault rocks and fault mechanisms. *Journal of the Geological Society* **133**, 191-213.

SIBSON R. H. 1995. Selective fault reactivation during basin inversion potential for fluid redistribution through fault-valve action. *Geological Society Special Publications* **88**, 3-19.

SIBSON R. H. 1998. Brittle failure mode plots for compressional and extensional tectonic regimes. *Journal of Structural Geology* **20**, 655-660.

SIBSON R. H. 2000. Tectonic controls on maximum sustainable overpressure: fluid redistribution from stress transitions. *Journal of Geochemical Exploration* **69–70**, 471-475.

SIBSON R. H. 2004. Controls on maximum fluid overpressure defining conditions for mesozonal mineralisation. *Journal of Structural Geology* **26**, 1127-1136.

TASSONE D. 2014 Compressional Deformation and Exhumation in Sedimentary Basins at 'Passive' continental Margins, with implications for hydrocarbon exploration and development. The Australian Shool of Petroleum. pp. 98. The University of Adelaide.

TWISS R. J. & M.MOORES E. 2007. Structural Geology. Structural Geology. Susan Finnemore Brennan, Second ed.

VIRGO S., ABE S. & URAI J. L. 2014. The evolution of crack seal vein and fracture networks in an evolving stress field: Insights from Discrete Element Models of fracture sealing. *Journal of Geophysical Research: Solid Earth* **119**, 8708-8727.

WILLCOX J. B. & STAGG H. M. J. 1990 Australia's southern margin a product of oblique extension. In LEVEN J. H.*, et al.* eds. pp. 269-281. Amsterdam: Amsterdam, Netherlands: Elsevier.

WILLIAMSON P. E., SWIFT M. G., O'BRIEN G. W. & FALVEY D. A. 1990. Two-stage Early Cretaceous rifting of the Otway Basin margin of southeastern Australia: Implications for rifting of the Australian southern margin. *Geology* **18**, 75-78.

APPENDIX A: GPS LOCATIONS

Table 1: GPS Locations where samples were taken from each location across the Otway Ranges.

Location	Latitude	Longitude
Wreck Beach	-38.7548	143.2128
Moonlight Head Transect	-38.7580	143.2148
- Castle Cove Location Adjacent Fault 1: **Castle Cove Location** **276West of Fault 2:**	-38.7823 38.7822	143.4264 143.4247
Crayfish Bay Transect	-38.8545	143.5373
Park-River Mouth	-38.8464	143.5608
Marengo	-38.7796	143.6660
Skenes Creek	-38.7256	143.7149
Smythes Creek	-38.7036	143.7618
Cumberland River	38.5766	143.9517
Lorne	-38.5491	143.9866

APPENDIX B: EXTENDED METHODS AND THIN SECTION PREPARATION

Materials:

Field Equipment and Laboratory Equipment:

- Field Notebook
- Compass clinometer
- GPS
- Hand lenses
- Field first Aid kit
- Measuring line
- Standard Rock hammer
- Mace
- Chisel
- Plastic sample bags
- Chalk
- Nikon Camera and Phone Camera
- Tape
- Masking Tape
- Permanent Marker – Red and Black
- Fracture samples from the Otway Basin (Calcite, Siderite, Quartz, open fractures)

- Cardboard cups
- Permanent marker
- Plastic sample bags
- Epoxy
- Epoxy Hardener
- Megapoxy H
- Megapoxy H hardener
- Rock Saw
- Electronics weights
- Pop stick
- Rubber Band
- Lab gloves
- Hair Tie
- Yellow sticky notes
- Camera
- Protective glasses
- Lab Coat
- Fracture samples (Calcite, Siderite, quartz and open)
- Tape

Sample preparation and measurements in the Field (Otway Basin – Victoria):

Samples of fracture fill cements were collected and prepared in the field in various locations across the Otway Basin along the Great Ocean Road coast of Victoria. Majority, if not all of the samples were taken from heavily weathered areas close to the the coast. All samples were taken from the Eumeralla Formation. Normally within metres of the ocean. The locations where samples were collected were as follows:

NOTE: Sample collection was to correlate from locations where fracture orientation data had already been collected previously. This involved facemaps. This was from Honours Thesis Josh Sage 2013. This was in order to make time spent in the field and data collection more efficient and to potentially relate geochemistry of fracture cement fills with fault and fracture networks and the implications for structural permeability.

Locations where samples were not taken but attended from can be seen in *Figure 1.*

Data Collection:

Specifically, samples were collected by walking out onto the wavecut platforms, assessing the fill of the fractures and then using the hammer and chisel to cut out the rock. Fracture orientation and dip was measured using the compass clinometer. Fracture orientation, aperture, type of fill and GPS location were recorded down in the field note book for each location and sample. The fractures would be marked and taped in order to keep the samples together due to their highly weathered states. They would then be placed in sample bags ready to be prepped in the lab. If there was a location that had limited data of fracture sets and orientation from Josh Sage Honours Thesis 2013 structural transects would be taken which involved data involved structural line transects as they passed across fracture planes from wavecut platforms and face maps (detailed cross sections of vertical rock face covering 2m 2 to 24m 2). In these transects and face maps, the orientations of fractures were measured using the compass clinometer. Further more we would attempt to take fracture samples from facemaps and transects already created in Sage 2013 thesis or Debenham 2016 PHd.

Transects were conducted at Crayfish Bay and Moonlight Head. Face-maps indirectly created for another project at Castle Cove.

Sample field preparation steps:

1. Travel to location. Check for previous data (facemaps, transects).
2. Create own data if necessary.
3. Identify fracture fill, aperture, orientation. Collect, number tape and sample.

   Place in sample bag. GPS location

   Format for input was:

Location	**GPS**			
Number (Recording)	**Dip/Dip Direction**	**Aperture**	**Description**	**Sample Number (If taken)**

4. Input data on computer (Excel).

Sample Preparation in the Lab (Sent off into thin sections) Mawson Building, University of Adelaide:

For the fracture fill samples to be sent off to (India) and cut into thin sections they first had to be moulded by Megapoxy H resin. This was conducted due to the samples being structurally weak from weathering (Ocean battering, rain and wind) and could break apart at any moment. The majority were too small to be cut directly into thin section sizes which is another reason why they had to be moulded into sufficient sizes. The samples were cut perpendicular to the fracture planes in order to see across the fracture plane.

Lab Preperation Steps:

1. Set up. Cardboard Cups, samples for Otway Basin, electronic scales.
2. Place selected sample (based on best fracture fill) in cup.
3. Take off tape if able.
4. Note orientation and sample number on cup.
5. Depending on size of sample measured out appropriate volume of Megapoxy H, and Megapoxy H hardener using the electronic scales. Varies between 100ml and 200ml batches. Ratio of resin to hardener of Megapoxy H is 3:1.
6. Stirred resin and hardener for at least 2 minutes or until no more streaks.
7. Poured Megapoxy H into rock sample cardboard cup until filled upon desired level.
8. Waited minimum 24 hours for Megapoxy H to harden.
9. Once the samples were set. Begin cutting the samples perpendicular to fracture orientation to be sent off into thin sections.

Fracture samples setting in Megapoxy H. 48hr Set time then cut using the Rock Saw

Lab Machines (Instrumentation):

Rock Saw (Large): The Rock saw was utilised once the weathered fracture samples were set in the Epoxy resin and ready to cut.
Based of safe operating procedure University of Adelaide:
Protective equipment: Safety glasses, plastic apron, enclosed shoes and hearing protection.

1. Use hose to wash stage to remove dust and unwanted leftover rocks. Check to see if the stage moves freely.
2. Check if power is on. Turn the saw on with green button. If the machine does not start double check to see if red safety pattern is off.
3. Turn water on tap and make sure pressure is high enough to clean the blade whilst cutting.
4. Pull stage out and place weathered fracture sample on stage. Make sure the rock is stable and the fracture orientation is perpendicular to the blade. Use the slit in the stage as an indication for where the blade will make its cut.
5. Place heels of your hands on stage and your fingers forward (not inwards) whilst holding the sample.
6. Gently push the stage until the rock meets the blade. Push with more effort once the rock is getting cut by the blade. Hold the sample in position. Make sure the blade does

not slip. If the blade stops immediately press red safety button. Wait before all movements cease and restart operating procedure.
7. Once the saw blade approaches end of cut, only small amounts of pushing are required. Allow the saw to cut the whole way through then pull stage out.
8. Remove rock pieces and continue if further cutting is required.
9. On completing of work turn off rock saw at the small red button. Turn off water supply.

Pictures: Calcite Fracture samples cut using the rock saw (Large).

Electronic Scales: Were utilised to measure volume by weight of the Megapoxy H resin. A cup would be placed on the electronic scales where the weight would then be "zeroed." Megapoxy H resin and hardener would then be measured out to the appropriate volume by weight to fill and set the subsequent sample. The weight is measured in grams.

Thin Sections: Thin sections were created by Continental Instruments, INDIA in

Megaepoxy H Resin Setup: Based of safe operating procedure University of Adelaide: Protective equipment: Safety glasses, white plastic apron, enclosed shoes, nitrile gloves:

Optical Microscope: Is used to conduct petrography of the samples. The optical microscope contains optional polarises in cross and plane polarised light. Each method results in different properties of the minerals to become observable. A rotating stage can change the variation of interaction between the polarisation of light which can also display different properties of the minerals.

1. Plug in microscope. Turn on lights source and set to desired level.
2. Place desired sample thin section on stage.
3. Use focusing adjuster to set the correct level of focus on the thin section.
4. Focus cross hairs and check if known minerals are behaving correctly.

5. Change light settings from plane polarised to cross polarised to observe different properties of the minerals.
6. Interpretations were made. Observing optical mineral properties revised according to (Kerr and Rogers 1977).

Computer Programs:

Analysis of structural data was completed using *Stereonet9* and *Georose* programs. These programs were used to interpret fracture sets and patterns in orientation.

Errors:

Field Work:
Measurements that were conducted in the Otway Basin were interpreted by the human eye and thus had a varying degree of error. Measurements that used the compass clinometer on average had a plus or minus 5 degrees of error when measuring dip orientation and dip angle. Aperture of fractures were "eye balled" and not measured directly with any instrument and likely had an error of plus or minus 2mm. When conducting transects the distance at which fractures were recorded using the measuring tape will have an error of plus or minus 1cm. Face-maps that were observed and drawn had the potential to be interpreted incorrectly and this measurement might have been off. Mineral identification of fracture cements was straight forward. Siderite fill was brown and weathered and easy to identify. Quartz and calcite however was more difficult, so generally when recording calcite or quartz we wrote down both. Confirmation if the mineral was calcite or quartz will be confirmed during petrography. Collection of rocks involved the taping, numbering of samples and placing in sample bags. There is a possibility of numbering the incorrect sample and sectioning it to a different outcrop or sample with a different orientation and fill.

Lab Work: Errors are most likely to occur in the preparation of samples and the cutting of sample rocks in to smaller sizes for thin section cutting. All preparations that has the potential for error:

1. Ratio of epoxy to hardener. The strict 3 to 1 ratio can be often misjudged, resulting in a resin mix that will not harden effectively.
2. Numbering of Samples.
3. The cutting of a sample may not adequately display the fracture of the sample. The rock saw must cut perpendicular to the fracture plane in order to display the texture of the fracture and for it to be analysed.

Petrography: Misidentification of mineral are a likely occurrence. The process involves a high degree of interpretation and depending on the viewer results can vary on fracture genesis and mechanical evolution. However, there is criteria to reduce the level of interpretation. All samples were taken from the Eumeralla Supersequence formation, a volcanogenic sedimentary rock. Quartz, alkali feldspar and plagioclase are probable. Siderite, calcite and quartz in the fractures are also to be expected (Sage, 2013).

Grain boundary Edges SEM (Misidentification of grains): Grain edges that are heavily deformed reflect a scatter that does not necessarily represent the specific mineral.

APPENDIX C: THIN SECTIONS PETROGRAPHY

These thin sections fractures samples observed using Optical Microscope and SEM. (Readings indicate Dip and dip direction)

*Indicates Josh Sage 2014 thin sections

Wreck Beach						
LFWB02 69/128	LFWB04 66/129	LFWB05 63/201				
Moonlight Head						
LFMH01 65/218	LFMH02 80/215	LFMH03 80/233	LFMH04 30/35	MH 04*		
Castle Cove						
LFCC02 21/144	LFCC03 76/291	LFCC04 71/018	LFCC05 60/129	LFCC07 88/195	LFCC09 86/195	LFCC11 50/180
LFCC1902 71/347	LFCC1903 080/220 074/346	CC 05*				
Crayfish Bay						
LFCB02 65/151						
Park River Mouth						
LFPM01 67/075	LFPM02 035/010					
Marengo						
LFM01 82/305						
Skenes Creek						
LFSK01 90/105	LFSK02 81/050					
Cumberland River						
CR01 78/020	CR02 88/090	CR 02*				
Lorne						
LFL01 42/200	LFL02 008/224					
Cape Otway						
CO 01*						

Table: Fracture Kinematics Characterisation (Dip/Dip Direction)

Crack-Seal calcite in-fill	Cross-cutting Siderite	Cataclastic Deformation	No Crack-Seal	Tensile Fracture Behaviour
LFMH02 - 065/218	LFCC1902 – 071/347 Cross cutting - orientation	LFCC02 – 021/144	LFPM01 - 067/075	LFCC1902 - 071/347
LFMH04 - 030/035	LFCC1903 – 080/220 and 074/346	LFCC03 – 076/291	LFCC1902 - 071/347	LFCC19CO3 - 080/220 and 074/346
LFL01 – 042/200	LFMH01 – 065/218	LFCC04 – 071/018	LFCC19CO3 - 080/220 and 074/346	LFMH01 – 065/218
LFL02 – 008/224	LFWB02 - 069/128	LFCC05 – 060/291	LFPM02- 035/010	LFMH02 - 065/218
LFMH01 – 065/218	LFWB04 - 066/129	LFCC07 - 088/195		LFMH04 - 030/035
MH-04 -	LFWB05 - 063/201	LFCC09- 86/ 195		LFWB02 - 069/128
CO-01 -	LFPM01 - 067/075	LFCC11- 50/180		LFWB04 - 066/129
	LFPM02 - 035/010	LFWB02 - 069/128		LFWB05 - 063/201
	CR01 - 078/020	LFWB04 - 066/129		LFCB02 - 065/151
	LFL01 - 042/200	LFCB02 - 065/151		LFPM01 -067/075
	LFL02 - 008/224	LFM01 – 067/075		LFPM02 - 035/010
		LFSK01- 090/105		CR01 -078/020
		LFSK02 - 081/050		LFL01-042/200
		CR02 -		LFL02 -008/224

Graphs: Fracture Locations, Aperture Size and Cement Fill Patterns

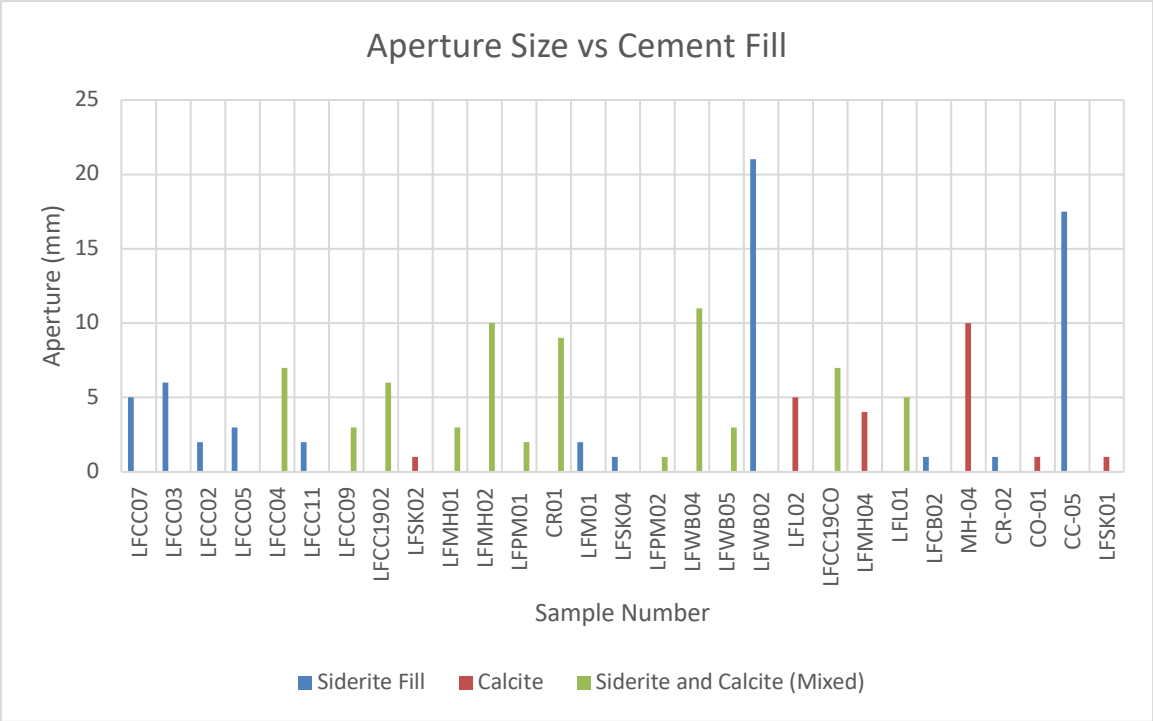

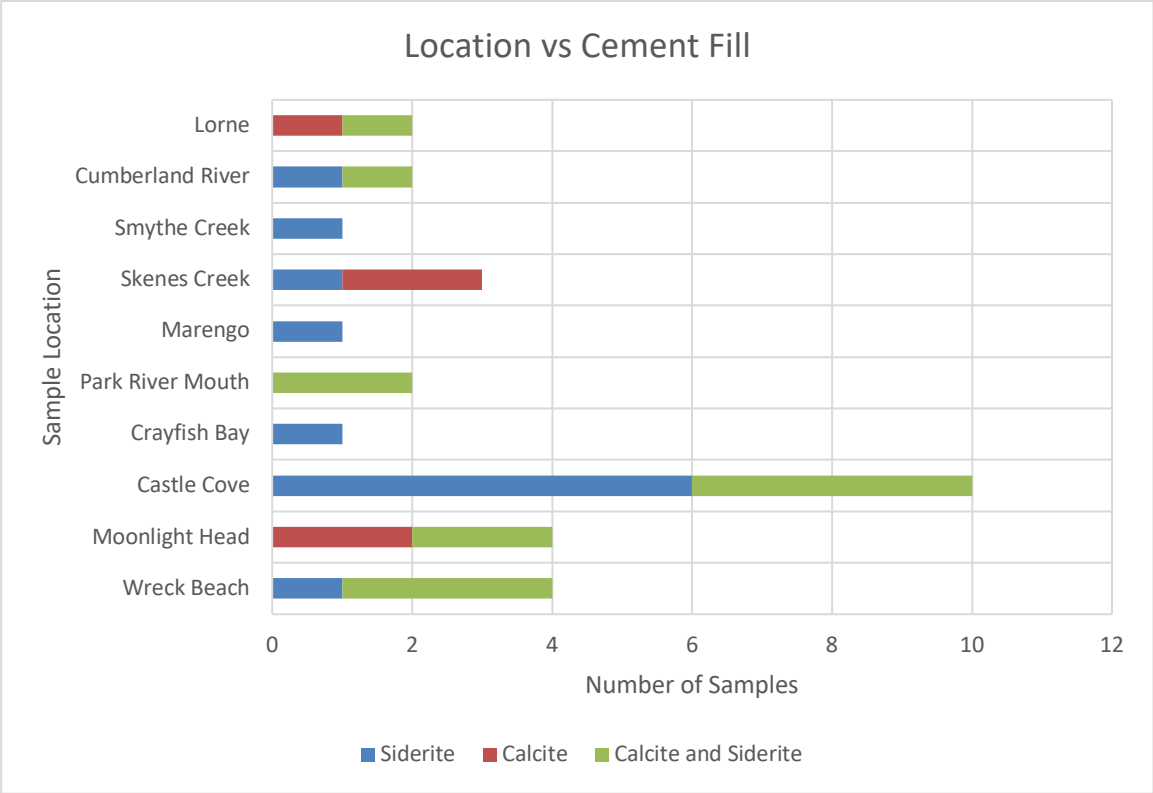

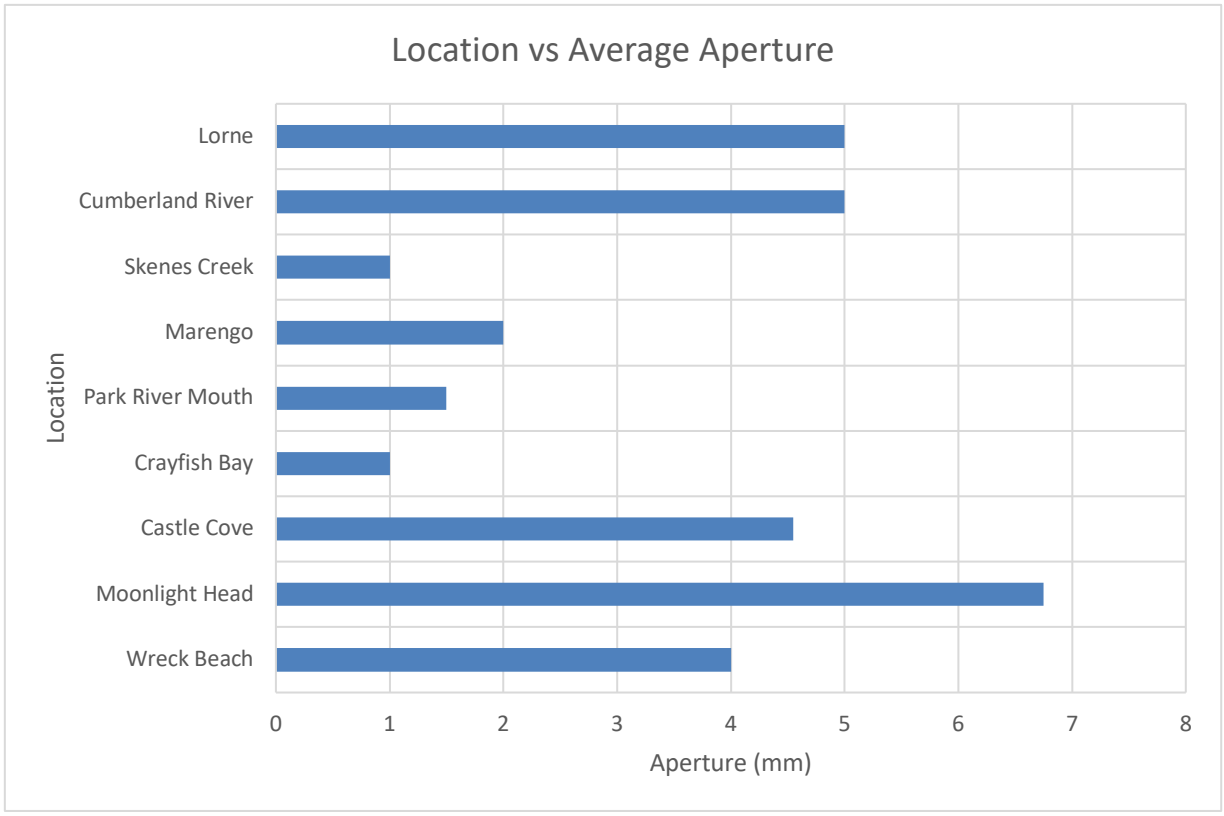
Location vs Average Aperture
Lorne
Cumberland River
Skenes Creek
Marengo
Park River Mouth
Crayfish Bay
Castle Cove
Moonlight Head
Wreck Beach
Location
0
1
2
3
4
5
6
7
8
Aperture (mm)

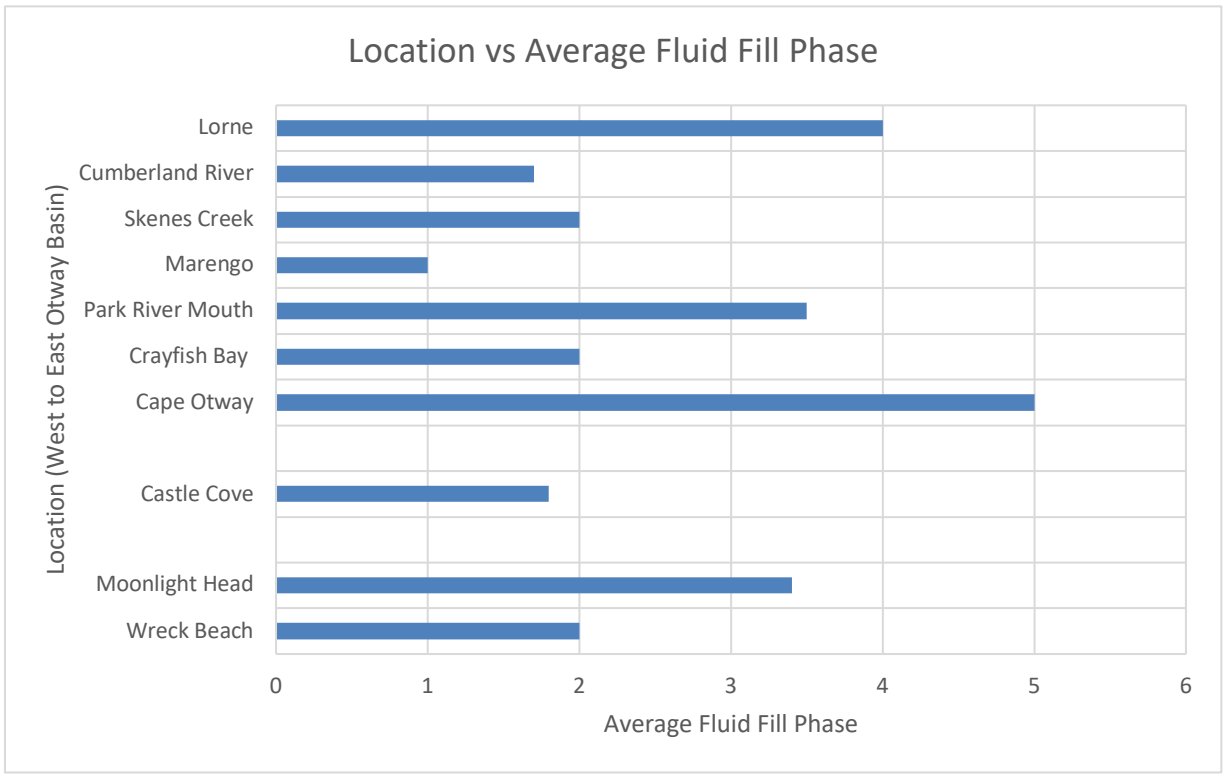
Location vs Average Fluid Fill Phase
Lorne
Cumberland River
Skenes Creek
Marengo
Park River Mouth
Crayfish Bay
Cape Otway
Castle Cove
Moonlight Head
Wreck Beach
Location (West to East Otway Basin)
0
1
2
3
4
5
6
Average Fluid Fill Phase

APPENDIX D: RAW FIELD MEASUREMENTS

Cement Fill: S = Siderite C = Calcite Q = Quartz H = Halo
Aperture: C = Closed O = Open

Table 1. Wreck Beach

Number	Dip Angle	Dip Direction	Aperture	Cement Fill	Sample Number
1	062	067	<1mm-7cm	S	L.F.W.B.01
2	069	128	5cm-1mm	S	L.F.W.B.02
3	019	071	1mm	S	L.F.W.B.03
4	066	129	1mm-2cm	S	L.F.W.B.04
5	063	201	1mm	C/S	L.F.W.B.05

Table 2. Moonlight Head Transect:

Number	Dip Angle	Dip Direction	Aperture	Cement fill	Distance	Sample Number
Data A – B at 249 Degrees Strike						
1	024	210	2mm	Q/C	10	
2	068	211	<1mm	S	9.56	
3	065	218	2mm	Q/C-S/H	8.74	L.F.M.H.01
4	078	225	1-2mm	Q/C-S/H	8.38	
5	065	210	1mm	Q/C-S/H	8.15	
6	072	228	3-5mm	Q/C-S/H	8.1	
7	079	218	3cm	Q/C-S/H	7.94	
8	075	220	<1mm	S	7.67	
9	080	215	2mm-5cm	Q/C-S/H	7.42	L.F.M.H.02
10	078	228	5mm-1cm	Q/C-S/H	7.31	
11	082	224	1-2cm	Q/C-S/H	7.24	
12	076	235	1mm	Q/C	6.67	
13	068	240	1-3mm	Q/C-S/H	6.6	
14	090	200	1mm	Q/C	6.42	
15	090	198	1mm	Q/C	5.95	
16	090	212	<1mm	Q/C	5.65	
17	086	240	1-3mm	Q/C	5.49	
18	085	225	<1mm	Q/C	4.9	
19	080	190	<1mm	S - no H	4.69	
20	080	225	1mm	Q/C-S/H	4.46	
21	080	233	1-2mm	Q/C	3.97	L.F.M.H.03
22	075	245	1mm	Q/C	3.82	
23	080	222	1mm	Q/C	3.6	
24	078	210	1mm	Q/C	3.5	

25	078	245	1mm	Q/C-S/H	3.35	
26	076	218	<1mm	Q/C	3.3	
27	070	184	<1mm	S/H	2.74	
28	080	230	2mm	Q/C	2.26	
29	070	228	<1mm	S/H	1.4	
30	048	220	<1mm	S/H	1.1	
31	034	234	<1mm	S/H	0.65	
32	050	060	1mm	S/H	0.18	
33	044	045	1mm	S/H	0.12	
Data C-D at 154 Degrees Strike						
34	088/240	088/240	4mm	Q/C	10.36	
35	030/035	030/035	1mm	Q/C	10.07	L.F.M.H.04
36	029/032	029/032	1mm	SF	8.9	
37	040/035	040/035	<1mm	S/H	8	
38	088/038	088/038	1mm	Q/C-S	7.2	
39	078/028	078/028	1mm	Q/C-S	6.15	
40	074/028	074/028	1mm	Q/C - S	5.42	
41	071/034	071/034	1mm	S/H	5.1	
42	078/224	078/224	<1mm	Q/C-S/H	4.1	
43	040/340	040/340	1-5mm	Q/C-S/H	3.67	L.F.M.H.05
44	044/178	044/178	<1mm	S/H	2.3	
45	052/214	052/214	<1mm	S/H	1.2	
46	084/180	084/180	<1mm	S/H	0.7	L.F.MH.06
47	070/184	070/184	<1mm	S/H	0.5	

Table 3: Face Map 1, Adjacent Fault Castle Cove

Number	Dip Angle	Dip Direction	Aperture	Cement fill	Sample Number
1	44	319	< 1	Siderite	
2	09	195	< 1	Siderite	
3	39	210	1	Siderite	
4	59	152	< 1	Siderite	
5	32	248	3	Siderite	
6	43	120	< 1	Siderite	
7	46	246	< 1	Siderite	
8	21	010	< 1	No fill	
9	40	248	< 1	Siderite	
10	41	185	2	Siderite	
11	38	235	< 1	Siderite	
12	70	138	< 1	Siderite	
13	63	018	< 1	Siderite	
14	68	002	2	Siderite	
15	72	091	< 1	Siderite	

16	46	179	< 1	Siderite	
17	40	030	< 1	Siderite	
18	19	078	2	Siderite	
19	59	350	40	Siderite	
20	78	100	1	Siderite	
21	20	238	< 1	Siderite	
22	48	322	< 1	Siderite	
23	16	004	< 1	Siderite	
24	71	019	1	Siderite	
25	71	018	20	Siderite	L.F.C.C.04
26	10	019	< 1	Siderite	
27	80	147	< 2	Siderite	
28	41	270	< 3	Siderite	
29	60	140	< 4	Siderite	
30	32	321	2	Siderite	
31	59	160	< 1	Siderite	
32	50	321	< 1	No fill	
33	45	145	< 1	No fill	
34	52	355	< 1	Siderite	
35	58	222	< 1	Siderite	
36	63	275	< 1	Siderite	
37	64	002	< 1	Siderite	
38	78	321	< 1	Siderite	
39	58	359	1	Siderite	
40	81	241	< 1	No fill	
41	44	339	1	Siderite	
42	69	160		No fill	
43	71	281	3-5	Siderite	
44	25	000	< 1	Siderite	
45	44	140		No fill	
46	50	108	2	Siderite	
47	44	289	1	Siderite	
48	51	128	< 1	Siderite	
49	39	348	1-10	Siderite	
50	81	267		No fill	
51	23	141	2	Siderite	
52	64	250	< 1	Siderite	
53	43	140	1-2	Siderite	
54	30	190	1	Siderite	
55	39	322	< 1	Siderite	
56	54	138	1	Siderite	
57	30	122	< 1	Siderite	
58	77	186		No fill	
59	22	002	< 1	Siderite	
60	79	255		No fill	
61	80	262		No fill	
62	03	211	< 1	Siderite	

63	38	349	< 1	Siderite	
64	49	330	1-2	Siderite	
65	38	331	1-3	Siderite	
66	18	029	< 1	Siderite	
67	30	352	5-20	Siderite	
68	58	154	1-2	Siderite	
69	51	162	< 1	Siderite	
70	30	319	< 1	Siderite	
71	22	242		No fill	
72	46	129		No fill	
73	80	268	< 1	Siderite	
74	76	268	< 1	Siderite	
75	30	007	< 1	Siderite	
76	65	309	< 1	No fill	
77	18	031	< 1	Siderite	
78	79	269		No fill	
79	83	295	< 1	Siderite	
80	20	325	< 1	Siderite	
81	19	345	< 1	Siderite	
82	78	129		No fill	
83	80	275		S	L.F.C.C.01
84	021	144		S	L.F.C.C.02
85	076	291		S	L.F.C.C.03
86	129	129		S eroded	L.F.C.C.05
87	300	300			L.F.C.C.06

Table 4: Castle Cove Away from fault:

Number	Dip	Dip Direction	Aperture	Cement Fill	Sample Number
1	29	220	1	?	
2	88	140		No fill	
3	30	220		No fill	
4	68	190		No fill	
5	79	192		No fill	
6	88	178		No fill	
7	40	169		No fill	
8	44	202		No fill	
9	86	151		No fill	
10	19	259		No fill	
11	89	190		No fill	
12	88	198		No fill	
13	19	277		No fill	
14	62	018		No fill	
15	59	305		No fill	
16	88	194	1-5	Siderite	

17	38	169		No fill	
18	49	185	< 1	Siderite	
19	88	175		No fill	
20	61	022		No fill	
21	14	128		No fill	
22	80	055		No fill	
23	36	001		No fill	
24	88	195	< 1	Siderite	LFCC07
25	40	185		No fill	
26	26	022	< 1	Siderite	
27	60	342		No fill	
28	61	341		No fill	
29	32	181		No fill	
30	48	185	1-2	Siderite	LFCC08
31	86	195	< 1	Siderite	LFCC09
32	88	202	< 1	Siderite	
33	53	245	1-3	Siderite	
34	38	005	< 1	Siderite	
35	18	125		No fill	
36	53	245	1	Siderite	
37	61	228	1	Siderite	
38	59	320		No fill	
39	65	241	< 1	Siderite	
40	16	128		No fill	
41	16	143		No fill	
42	42	048	< 1	Siderite	
43	42	008	< 1	Siderite	
44	68	220		No fill	
45	58	318	< 1	Siderite	
46	54	226	< 1	Siderite	
47	46	220	< 1	Siderite	
48	48	000		No fill	
49	58	195	1-2	Siderite	LFCC10
50	57	190	1	Siderite	
51	36	045		No fill	
52	88	009		No fill	
53	38	248	< 1	Siderite	
54	50	260	< 1	Siderite	
55	78	019		No fill	
56	62	222	0-5	Siderite	
57	53	198	< 1	Siderite	
58	57	192	< 1	No fill	
59	50	180	< 1	Siderite	LFCC11
60	79	003	1	No fill	
61	59	051	1	No fill	
62	070	340	<1mm - 1cm	C/Q	LFCC1901

63	071	347	1-3mm	S/H - Q/C	LFCC1902
64	080	220	1mm	S/H - C/Q	LFCC1903
65	074	346	1mm	S/H - C/Q	LFCC1903
66	078	315	1-2mm	C	LFCC1904

Table 5: Crayfish Bay Transect

Number	Dip	Dip Direction	Aperture	Cement Fill	Sample Number
A-B Striking North South					
1	068	328	OAS	NF	
2	059	220	<1mm	NF	L.F.C.B.04
3	022	308	OAS	NF	
4	070	045	<1mm	S	
5	087	158	C	NF	
6	055	127	C	S/H	
7	058	145	C	S/H	
8	063	358	C	NF	
9	080	340	C	S/H	
10	064	340	C	weak H	
11	044	045	OAS	NF	
12	056	142	OAS - 3mm	NF	
13	061	138	OAS - 5mm	NF	
14	071	129	C	S/H	
15	070	130	C	S/H	L.F.C.B.03
16	065	151	OAS - <1mm	S/H	L.F.C.B.02
C-D Striking East West					
1	058	314	C	C	L.F.C.B.05
2	050	031	C	C	
3	086	342	C	C	
4	068	144	C	C	
5	067	142	C	C	
6	016	331	C	C	
7	064	143	C	C	
8	090	050	C	C	
9	076	030	OAS	OAS	
10	063	126	C	C	
11	064	142	C	C	L.F.C.B.01
12	080	148	C	C	L.F.C.B.05
13	082	222	C	C	
14	089	152	C	C	

Table 6: Park River – Mouth

Number	Dip	Dip Direction	Aperture	Cement Fill	Sample Number
1	067/075	067/075	3mm	Ca - S/H 15cm	L.F.P.M.01
2	035/010	035/010	1mm	Ca - S/H 15mm	L.F.P.M.02

Table 7: Marengo

Number	Dip	Dip Direction	Aperture	Cement Fill	Sample number
1	082	305	2mm	siderite	L.F.M.01
2	083	125	<1mm	siderite weathered	L.F.M.02

Table 8: Skenes Creek

Number	Dip	Dip Direction	Aperture	Cement Fill	Sample number
1	090	105	<1mm	S	L.F.SK.01
2	081	050	2mm	C	L.F.SK.02
3	083	245	1mm	S	L.F.SK.03
4	079	079	3mm +<1mm	S	L.F.SK.04
5	068	000	2-3 1 mill fills + 2cm wide halo	S	L.F.SK.05

Table 9: Smythes Creek

Number	Dip	Dip Direction	Aperture	Cement Fill	Sample number
1	059	260	1-5mm	S - Minimal H	L.F.S.C.01

Table 10: Cumberland River

Number	Dip	Dip Direction	Aperture	Cement Fill	Sample number
1	078	020	<1mm	siderite	LFCR01
2	088	090	1mm	siderite	LFCR02

Table 11: Lorne

Number	Dip	Dip Direction	Aperture	Cement Fill	Sample number
1	042	200	2-3mm	Q/C	L.F.L.01
2	008	224	3-5mm	Q/C - SE set	L.F.L.02

APPENDIX E: GEOCHEMISTRY

Geochemistry GXMAP Elemental Abundance Summary of Fracture Cements:

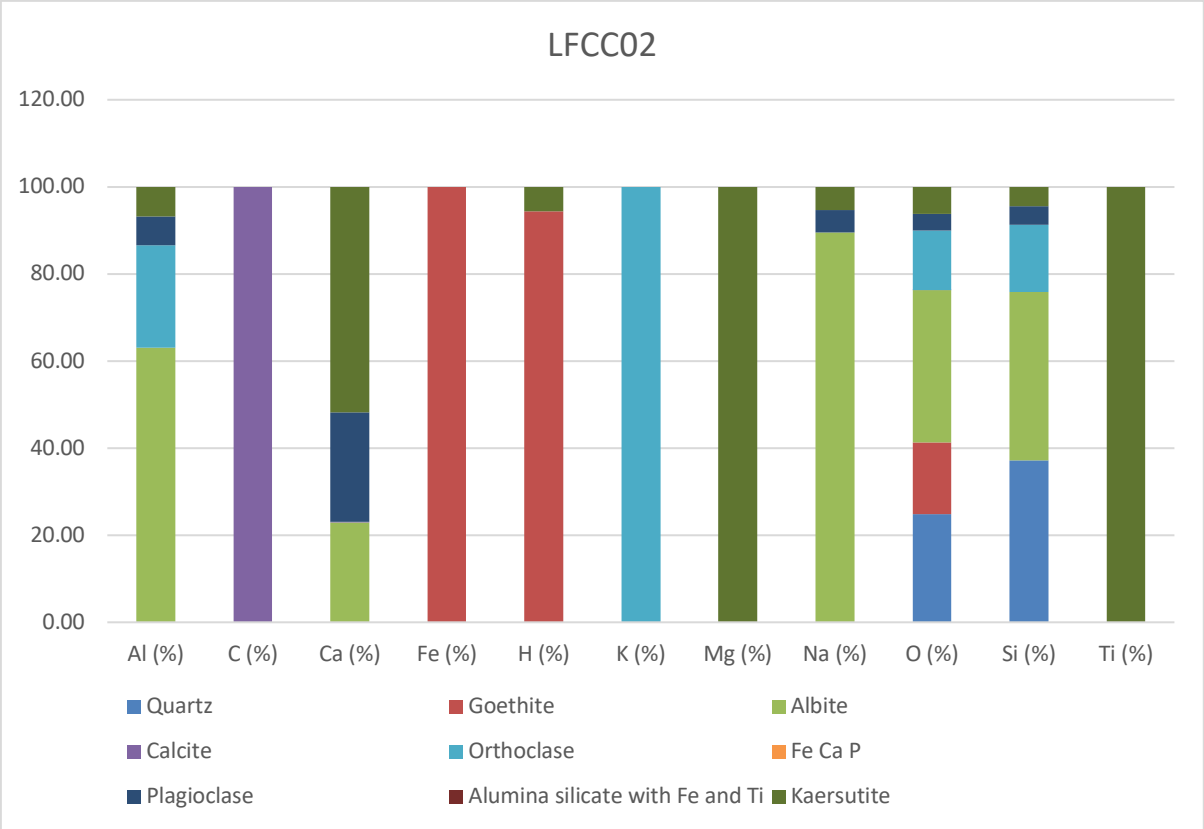

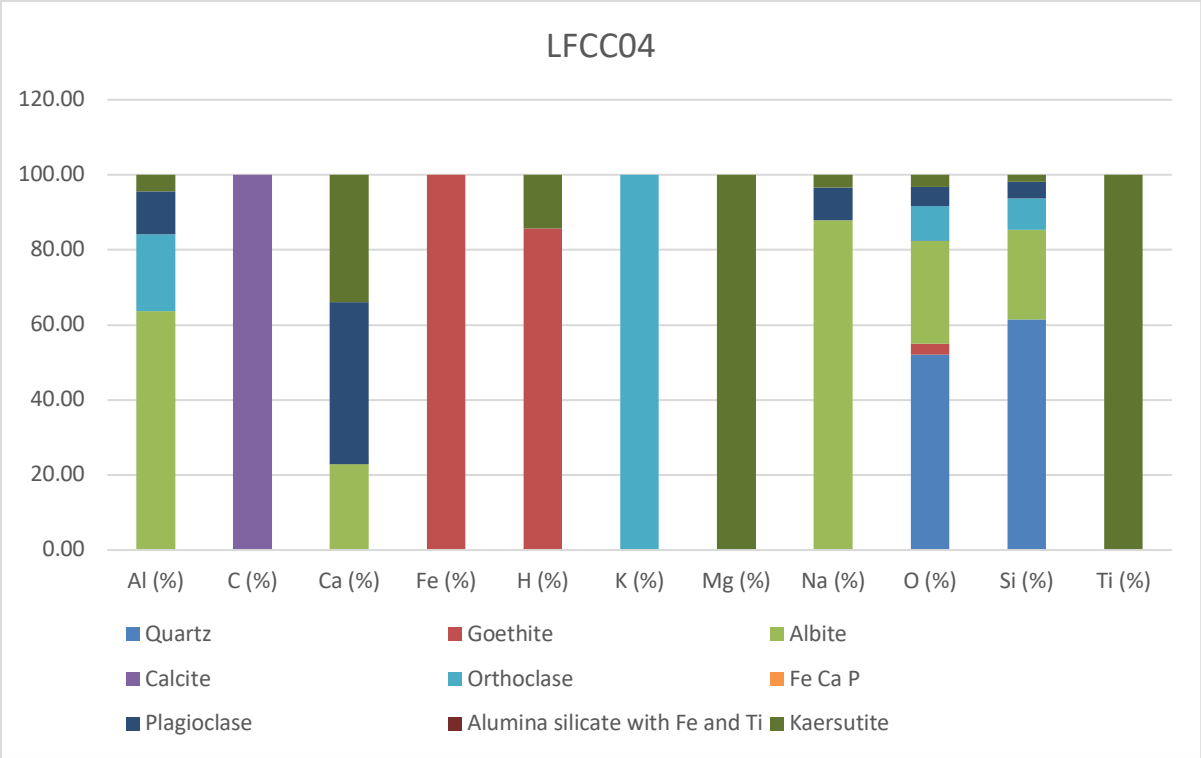
LFCC04
120.00
100.00
80.00
60.00
40.00
20.00
0.00
Al (%)
C (%)
Ca (%)
Fe (%)
H (%)
K (%)
Mg (%)
Na (%)
O (%)
Si (%)
Ti (%)
Quartz
Goethite
Albite
Calcite
Orthoclase
Fe Ca P
Plagioclase
Alumina silicate with Fe and Ti
Kaersutite

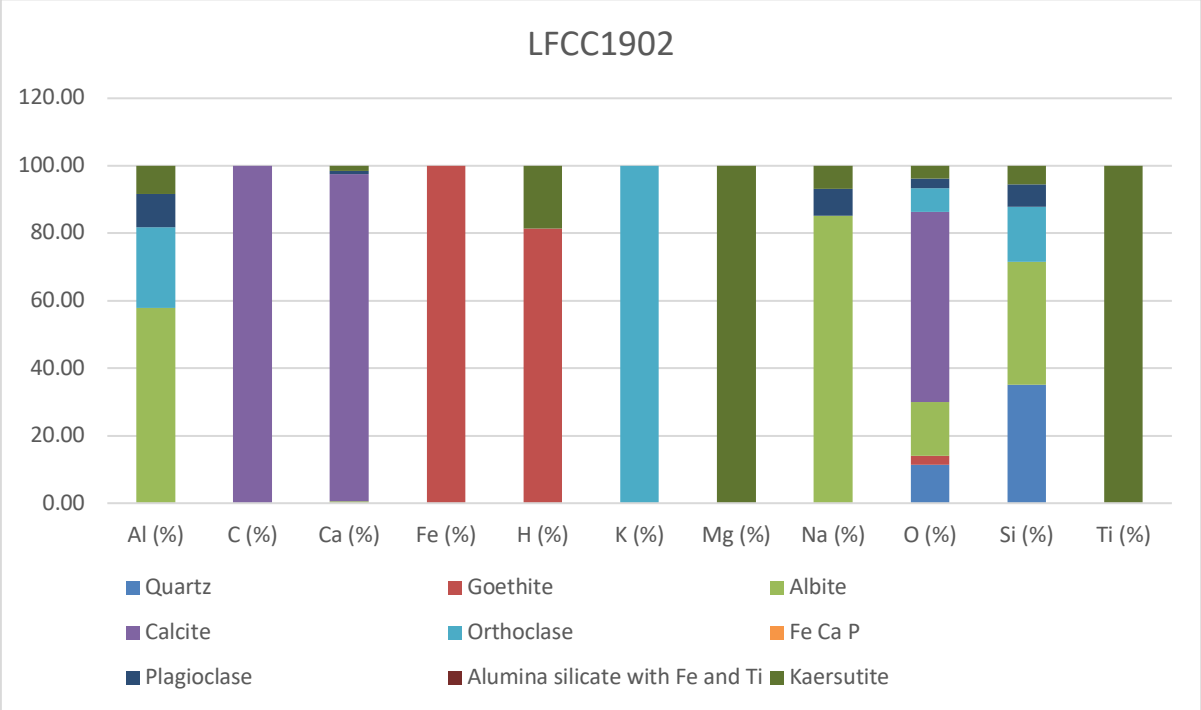
LFCC1902
120.00
100.00
80.00
60.00
40.00
20.00
0.00
Al (%)
C (%)
Ca (%)
Fe (%)
H (%)
K (%)
Mg (%)
Na (%)
O (%)
Si (%)
Ti (%)
Quartz
Goethite
Albite
Calcite
Orthoclase
Fe Ca P
Plagioclase
Alumina silicate with Fe and Ti
Kaersutite

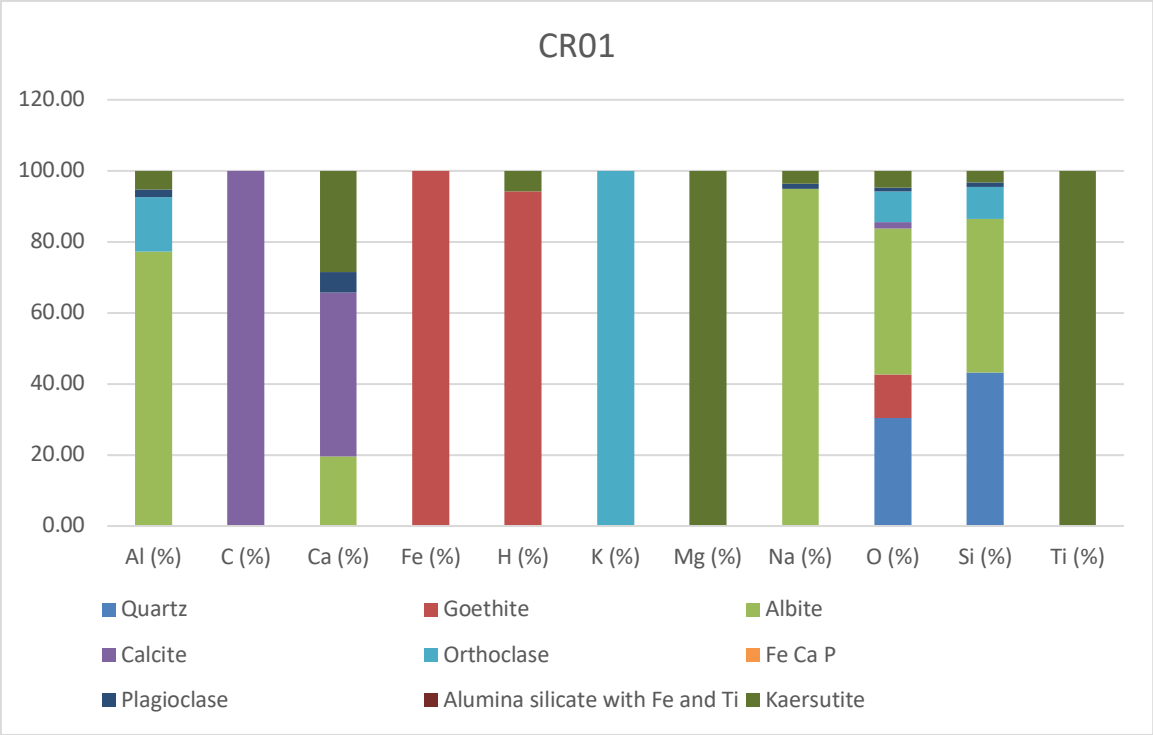
CR01
120.00
100.00
80.00
60.00
40.00
20.00
0.00
Al (%)
C (%)
Ca (%)
Fe (%)
H (%)
K (%)
Mg (%)
Na (%)
O (%)
Si (%)
Ti (%)
Quartz
Goethite
Albite
Calcite
Orthoclase
Fe Ca P
Plagioclase
Alumina silicate with Fe and Ti
Kaersutite

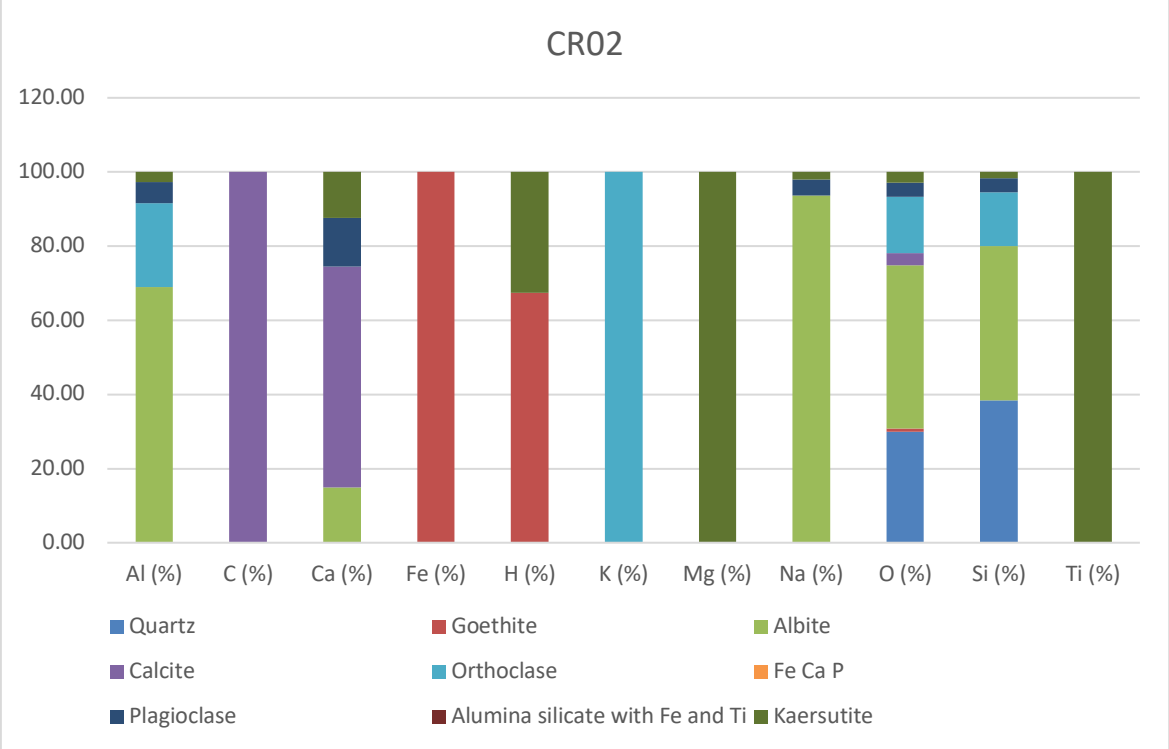
CR02
120.00
100.00
80.00
60.00
40.00
20.00
0.00
Al (%)
C (%)
Ca (%)
Fe (%)
H (%)
K (%)
Mg (%)
Na (%)
O (%)
Si (%)
Ti (%)
Quartz
Goethite
Albite
Calcite
Orthoclase
Fe Ca P
Plagioclase
Alumina silicate with Fe and Ti
Kaersutite

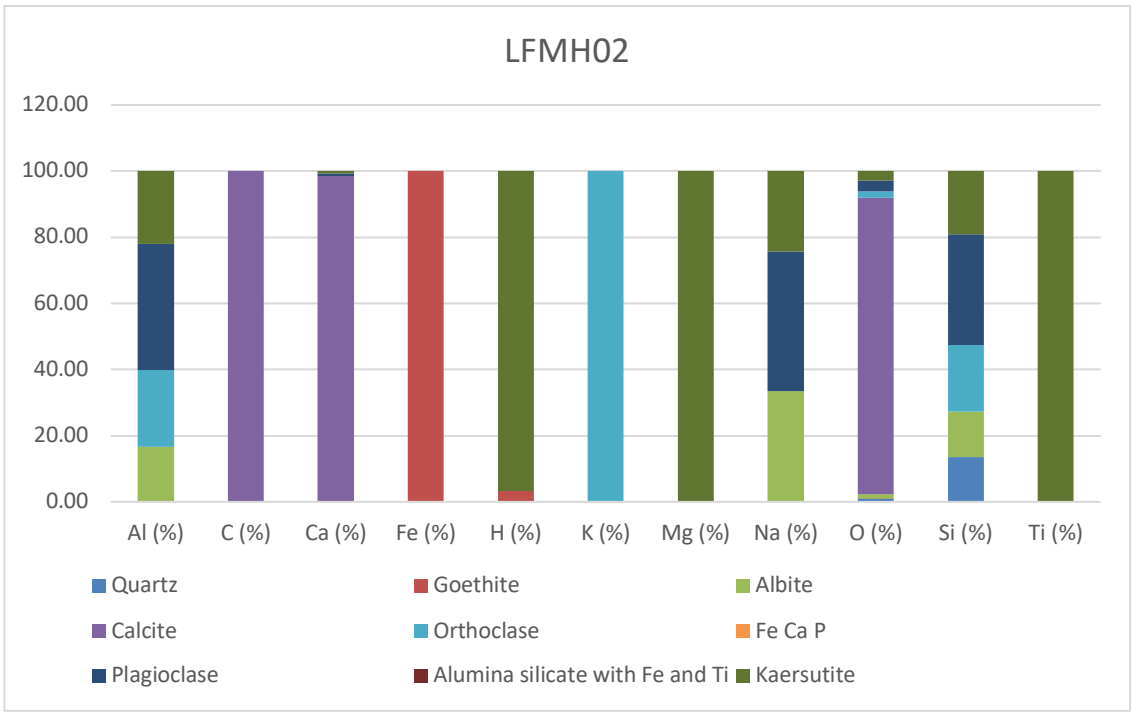
LFMH02
120.00
100.00
80.00
60.00
40.00
20.00
0.00
Al (%)
C (%)
Ca (%)
Fe (%)
H (%)
K (%)
Mg (%)
Na (%)
O (%)
Si (%)
Ti (%)
Quartz
Goethite
Albite
Calcite
Orthoclase
Fe Ca P
Plagioclase
Alumina silicate with Fe and Ti
Kaersutite

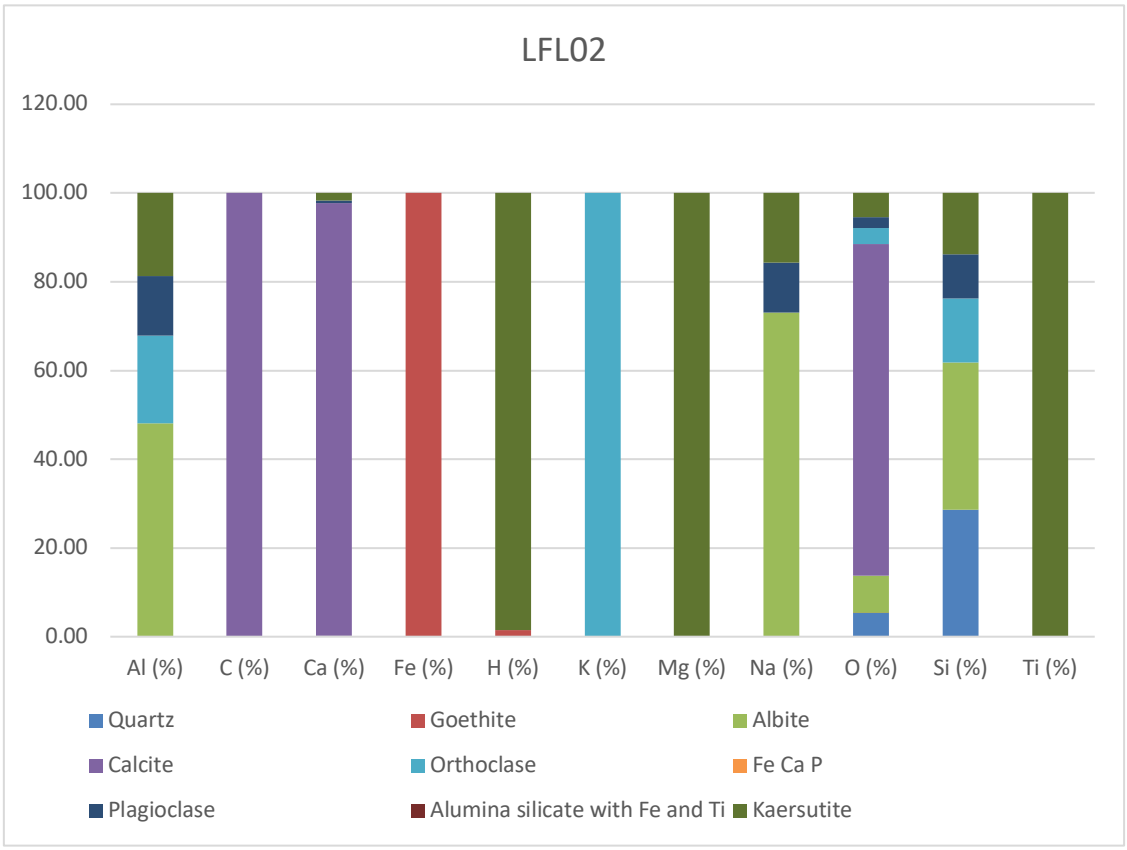
LFL02
120.00
100.00
80.00
60.00
40.00
20.00
0.00
Al (%)
C (%)
Ca (%)
Fe (%)
H (%)
K (%)
Mg (%)
Na (%)
O (%)
Si (%)
Ti (%)
Quartz
Goethite
Albite
Calcite
Orthoclase
Fe Ca P
Plagioclase
Alumina silicate with Fe and Ti
Kaersutite

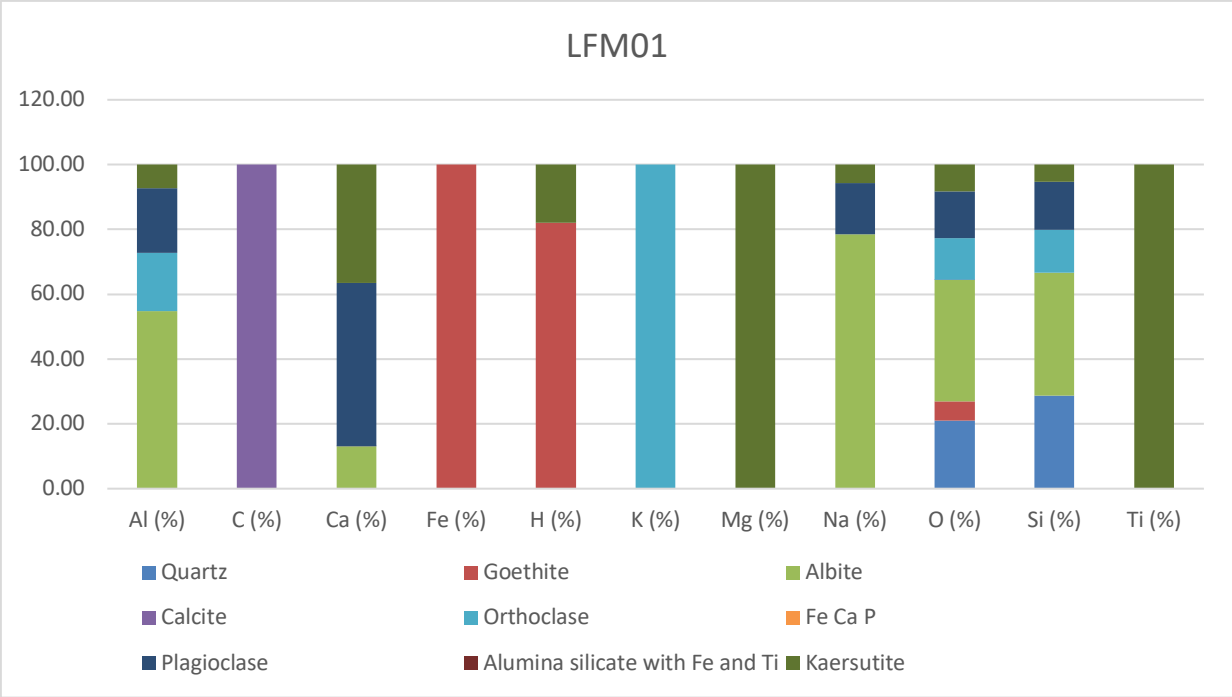
LFM01
120.00
100.00
80.00
60.00
40.00
20.00
0.00
Al (%)
C (%)
Ca (%)
Fe (%)
H (%)
K (%)
Mg (%)
Na (%)
O (%)
Si (%)
Ti (%)
Quartz
Goethite
Albite
Calcite
Orthoclase
Fe Ca P
Plagioclase
Alumina silicate with Fe and Ti
Kaersutite

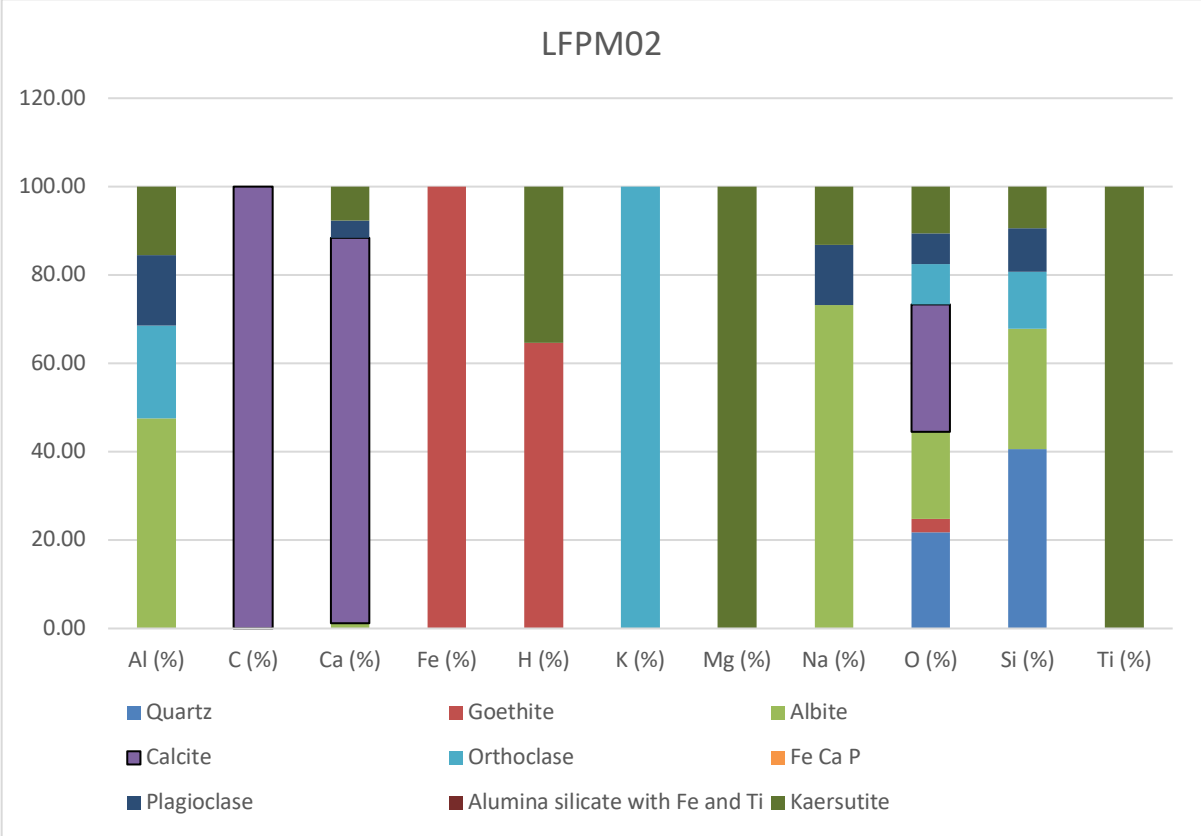
LFPM02
120.00
100.00
80.00
60.00
40.00
20.00
0.00
Al (%)
C (%)
Ca (%)
Fe (%)
H (%)
K (%)
Mg (%)
Na (%)
O (%)
Si (%)
Ti (%)
Quartz
Goethite
Albite
Calcite
Orthoclase
Fe Ca P
Plagioclase
Alumina silicate with Fe and Ti
Kaersutite

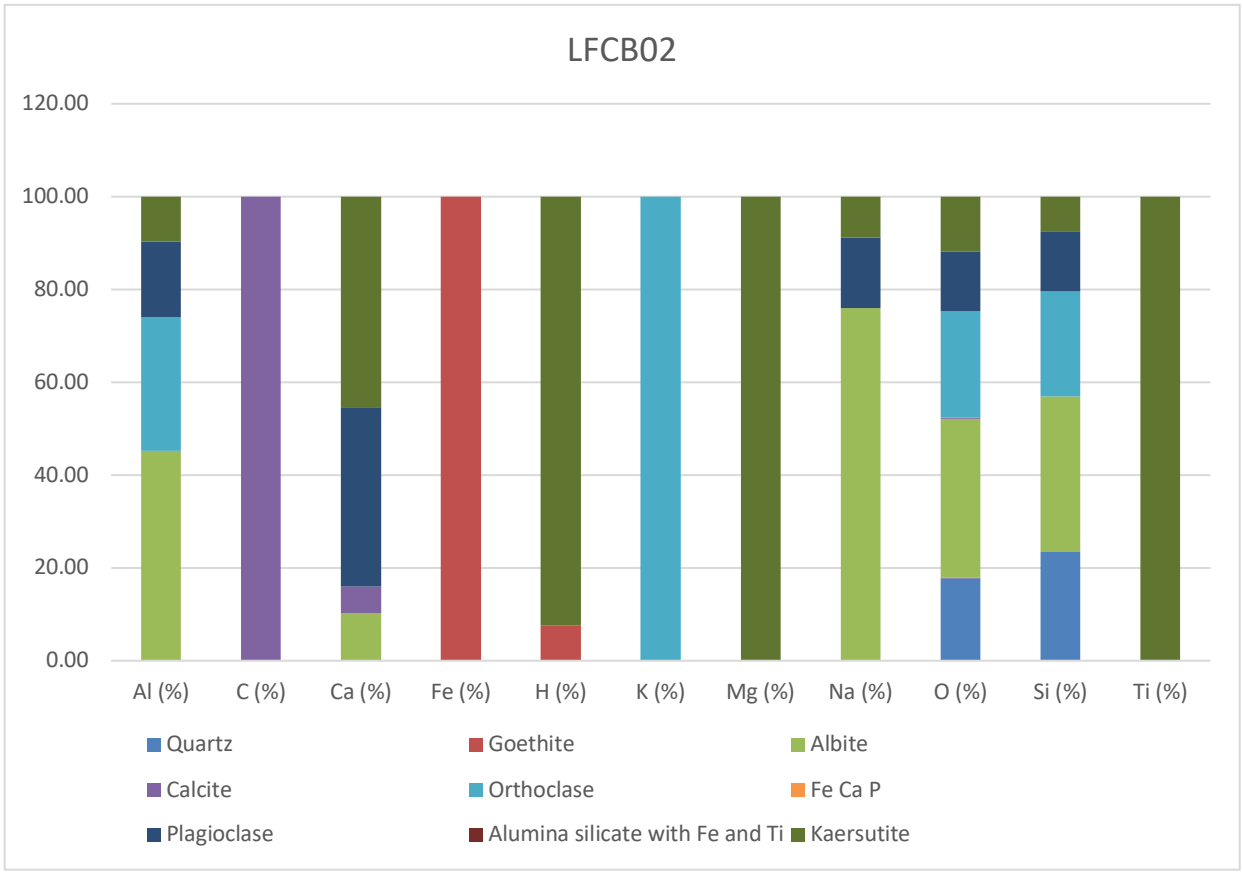
LFCB02
120.00
100.00
80.00
60.00
40.00
20.00
0.00
Al (%)
C (%)
Ca (%)
Fe (%)
H (%)
K (%)
Mg (%)
Na (%)
O (%)
Si (%)
Ti (%)
Quartz
Goethite
Albite
Calcite
Orthoclase
Fe Ca P
Plagioclase
Alumina silicate with Fe and Ti
Kaersutite

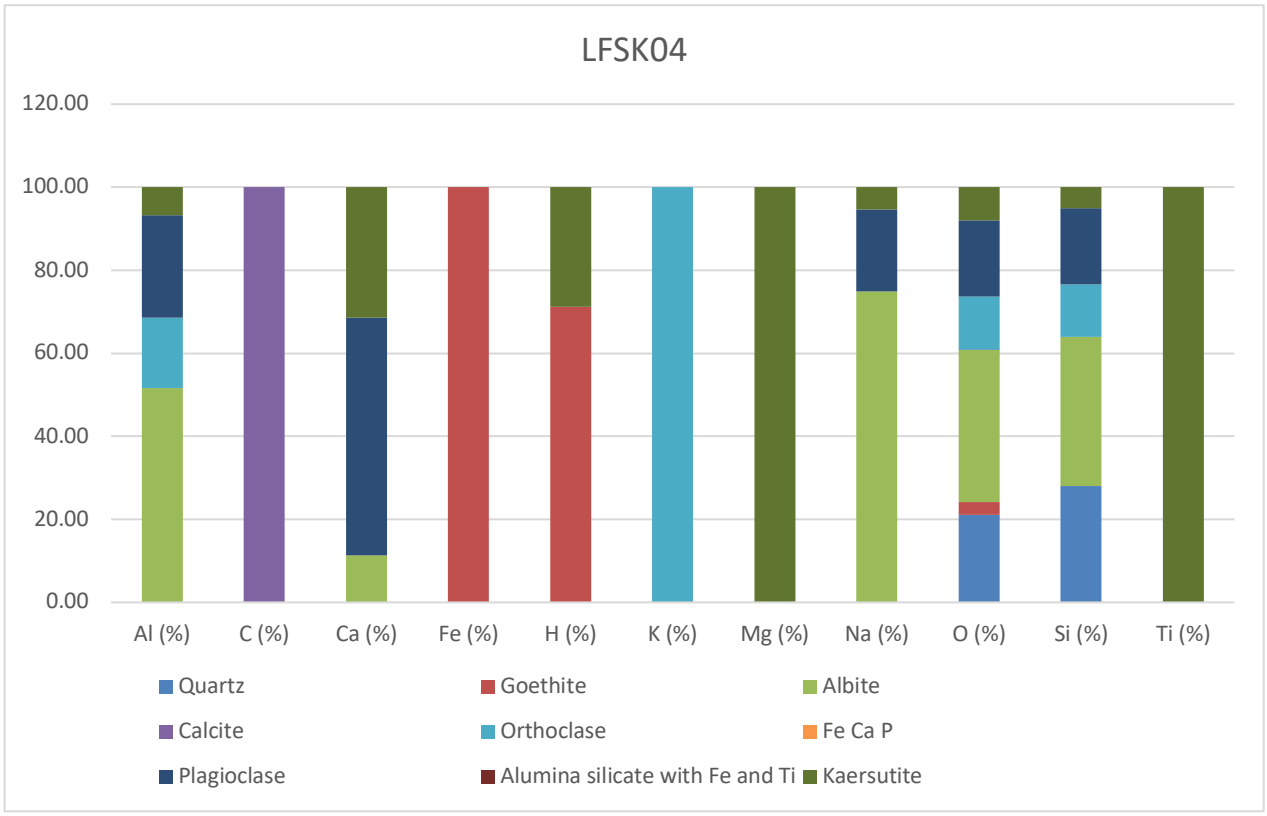
LFSK04
120.00
100.00
80.00
60.00
40.00
20.00
0.00
Al (%)
C (%)
Ca (%)
Fe (%)
H (%)
K (%)
Mg (%)
Na (%)
O (%)
Si (%)
Ti (%)
Quartz
Goethite
Albite
Calcite
Orthoclase
Fe Ca P
Plagioclase
Alumina silicate with Fe and Ti
Kaersutite

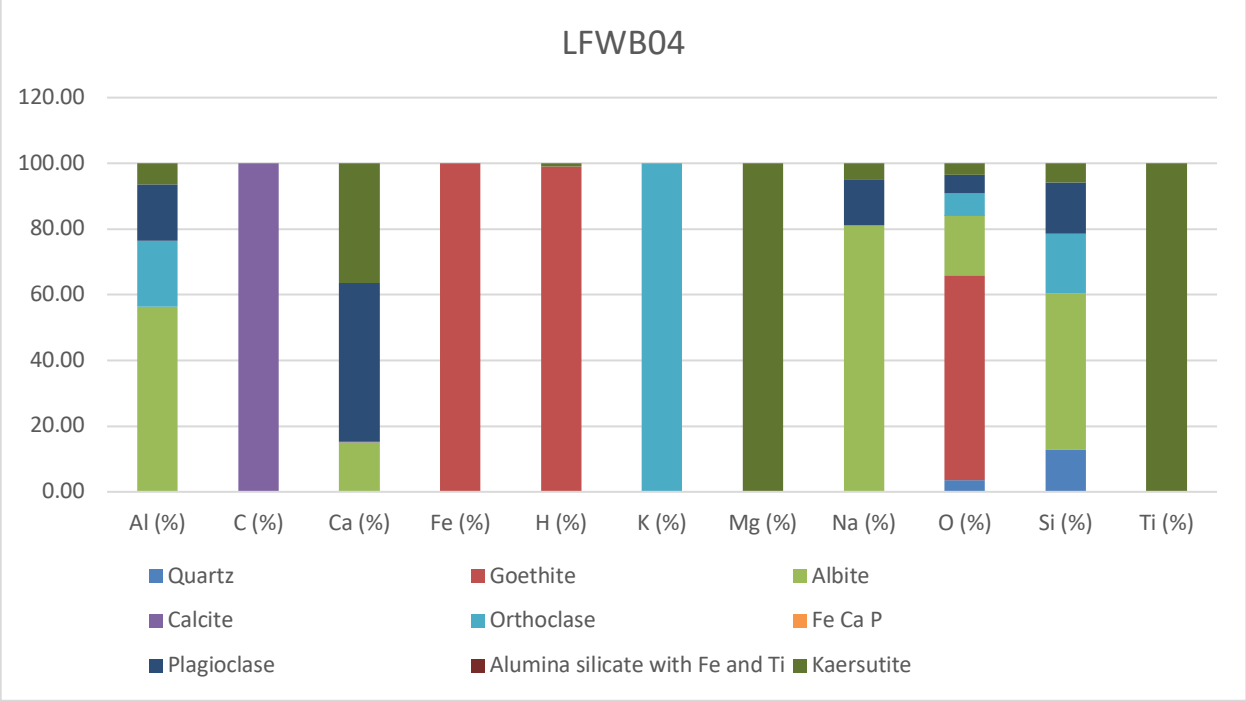
LFWB04
120.00
100.00
80.00
60.00
40.00
20.00
0.00
Al (%)
C (%)
Ca (%)
Fe (%)
H (%)
K (%)
Mg (%)
Na (%)
O (%)
Si (%)
Ti (%)
Quartz
Goethite
Albite
Calcite
Orthoclase
Fe Ca P
Plagioclase
Alumina silicate with Fe and Ti
Kaersutite